

NOTE TO USERS

This reproduction is the best copy available.

UMI[®]

AN EXPERIMENTAL STUDY OF MIDDLE-EAR
VIBRATIONS IN RATS

Fadi G. Akache
Department of BioMedical Engineering
McGill University
Montréal, Canada
May 2005

A thesis submitted to McGill University in partial
fulfilment of the requirements of the degree
of Master of Engineering.

©Fadi G. Akache, 2005



Library and
Archives Canada

Bibliothèque et
Archives Canada

Published Heritage
Branch

Direction du
Patrimoine de l'édition

395 Wellington Street
Ottawa ON K1A 0N4
Canada

395, rue Wellington
Ottawa ON K1A 0N4
Canada

Your file *Votre référence*

ISBN: 0-494-12576-4

Our file *Notre référence*

ISBN: 0-494-12576-4

NOTICE:

The author has granted a non-exclusive license allowing Library and Archives Canada to reproduce, publish, archive, preserve, conserve, communicate to the public by telecommunication or on the Internet, loan, distribute and sell theses worldwide, for commercial or non-commercial purposes, in microform, paper, electronic and/or any other formats.

The author retains copyright ownership and moral rights in this thesis. Neither the thesis nor substantial extracts from it may be printed or otherwise reproduced without the author's permission.

AVIS:

L'auteur a accordé une licence non exclusive permettant à la Bibliothèque et Archives Canada de reproduire, publier, archiver, sauvegarder, conserver, transmettre au public par télécommunication ou par l'Internet, prêter, distribuer et vendre des thèses partout dans le monde, à des fins commerciales ou autres, sur support microforme, papier, électronique et/ou autres formats.

L'auteur conserve la propriété du droit d'auteur et des droits moraux qui protègent cette thèse. Ni la thèse ni des extraits substantiels de celle-ci ne doivent être imprimés ou autrement reproduits sans son autorisation.

In compliance with the Canadian Privacy Act some supporting forms may have been removed from this thesis.

Conformément à la loi canadienne sur la protection de la vie privée, quelques formulaires secondaires ont été enlevés de cette thèse.

While these forms may be included in the document page count, their removal does not represent any loss of content from the thesis.

Bien que ces formulaires aient inclus dans la pagination, il n'y aura aucun contenu manquant.


Canada

Abstract

Animal models are valuable tools in auditory research. Rats are potentially very useful for this purpose. They are low in cost, they are genetically similar to humans, and the middle-ear structures are easily approachable. The goal of the present study is to better characterize the mechanics of the rat middle ear by measuring frequency responses at multiple points on the tympanic membrane for the first time, and with better frequency resolution than in previous studies. A laser Doppler vibrometer was used to measure the vibrations. Measurements were done on seven rats. Tympanic membrane vibrations at seven different points, in the frequency range of 1 000 to 10 000 Hz, are presented. We provide a measure of the noise floor and investigate the linearity of the rat tympanic membrane. The repeatability of the rat's middle-ear response and inter-animal variability at the umbo are presented. The vibration modes of the tympanic membrane and manubrium are also investigated.

Résumé

Les modèles animaux sont des outils importants dans la recherche auditive. Les rats sont potentiellement très utiles à cet effet. Ils ne sont pas coûteux, ils sont génétiquement similaires aux humains et les structures de l'oreille moyenne sont facilement accessibles. Le but du présent travail est de mieux caractériser la mécanique de l'oreille moyenne du rat en mesurant les réponses de la membrane tympanique à diverses fréquences. Nous avons mesuré les réponses à plusieurs endroits sur le tympan pour la première fois et ce, avec une meilleure résolution que dans les études précédentes. Nous nous sommes servis d'un vibromètre à laser Doppler pour mesurer les vibrations. Les mesures ont été effectuées sur sept rats. Les vibrations du tympan ont été prises à sept endroits différents, dans la gamme de fréquence de 1000 à 10 000 Hz. Nous fournissons une mesure du seuil de bruit et examinons la linéarité de la membrane tympanique du rat. La répétitivité de la réponse de l'oreille moyenne du rat et la variabilité inter animale au niveau de l'umbo sont présentées. Les modes de vibration du tympan et du manubrium sont aussi étudiés.

Acknowledgements

I would like to thank my supervisor, Dr. W. Robert J. Funnell, for his guidance and patience. His merits as a supervisor are greatly appreciated.

I would also like to express gratitude to my co-supervisor, Dr. Sam Daniel, director of research for the division of Pediatric Otolaryngology at the Montreal Children's Hospital, for sharing with me his knowledge in the medical aspect of middle-ear research.

Many thanks go out to my friends and family for their endless support and encouragement.

This accomplishment is due in large part to everyone I have mentioned.

This work was supported by the Canadian Institutes of Health Research, the Natural Sciences and Engineering Research Council of Canada, the Fonds de Recherche en Santé du Québec, the Montreal Children's Hospital Research Institute and the McGill University Health Centre Research Institute.

Table of Contents

Abstract	i
Résumé	ii
Acknowledgements	iii
Table of Contents	iv
CHAPTER 1. Introduction.....	1
CHAPTER 2. Hearing and Anatomy.....	3
2.1 Introduction	3
2.2 Overview of Hearing.....	3
2.2.1 Sound	3
2.2.2 Perception.....	3
2.2.3 Sound Measurement	4
2.3 Temporal Bone.....	5
2.4 Human Middle Ear.....	6
2.4.1 Tympanic Membrane	6
2.4.2 The Ossicles	8
2.4.3 The Middle-Ear Muscles.....	8
2.4.4 The Tympanic Cavity	9
2.5 Rat Middle Ear	9
2.6 Axis of Rotation	12
2.7 Impedance Matching.....	15
CHAPTER 3. Laser Doppler Vibrometry	17
3.1 Introduction	17
3.2 Interferometry	17
3.3 Heterodyne Interferometry	18
3.3.1 Introduction	18
3.3.2 Laser Doppler Vibrometry	19
3.4 Conclusion	21
CHAPTER 4. Previous Studies	22
4.1 Introduction	22
4.2 Post Mortem Middle Ear	22
4.3 Rat Studies	26
4.4 Microtype Study.....	28
4.5 Motion of the Malleus.....	29
4.6 Conclusions	30

CHAPTER 5. Methodology	32
5.1 Introduction	32
5.2 Specimen Preparation	32
5.3 Acoustical System	33
5.4 Optical System	37
5.5 Signal Analysis	38
5.6 Investigations.....	41
5.6.1 Excitation Signal.....	41
5.6.2 Noise Floor	42
5.6.3 Linearity	42
5.6.4 Repeatability	43
5.6.5 Variability.....	46
5.6.6 Characterizing TM Vibrations.....	49
 CHAPTER 6. Results	 50
6.1 Introduction	50
6.2 Excitation Signal.....	50
6.3 Noise Floor.....	52
6.4 Linearity.....	53
6.5 Repeatability	55
6.6 Inter-Animal Variability at the Umbo.....	60
6.7 Characterizing Manubrial Vibrations	62
6.8 Characterizing TM Vibrations.....	68
 CHAPTER 7. Conclusions.....	 71
7.1 Summary.....	71
7.2 Future Work	72
7.2.1 Introduction	72
7.2.2 Experimental Methodology.....	72
7.2.3 Understanding of Middle-Ear Mechanics	73
 References.....	 75

CHAPTER 1. Introduction

Hearing impairment affects up to 30% of the population (emedicine.com). It is also one of the most common birth defects, affecting 6 in every 1 000 babies in Canada (thfc.ca). According to the Hearing Foundation of Canada, hearing loss is the third leading chronic disability after arthritis and hyperextension (thfc.ca). The middle ear plays a major role in the hearing process. There is still much about the ear that remains to be understood, and with a better understanding of the mechanics of the middle ear we shall be able to improve the diagnosis and treatment of hearing disorders.

It has been suggested by Hellström et al. (1982) that the rat is of value in otological research because the middle-ear structures are easily approachable and because rats are less expensive than other species used in middle-ear research. Since almost all human genes known to be associated with disease have orthologues in the rat genome, and with the recent addition of rats to the list of species whose genomes have been mapped (Rat Genome Sequencing Consortium, 2004), the rat could become an even more valuable tool in middle-ear research.

Few measurements have been done in the past to study rat middle-ear mechanics. Early studies by Beccari and Molinengo (1958) and by Ishii et al. (1964) reported the frequencies of maximum sensitivity of the ear, but no frequency responses were shown. Moreover, these researchers did not have access to today's more advanced measurement techniques. More recent studies by Doan et al. (1996) and Bigelow et al. (1996, 1998) did provide frequency responses and used technology similar to the one presented here, but they measured the frequency responses only at one point on the tympanic membrane.. To fully understand the vibrations of the middle ear, one needs to measure displacements at multiple points.

The goal of the present study is to better characterize the mechanics of the rat middle ear by measuring frequency responses at multiple points and with better frequency resolution. The method used is laser Doppler vibrometry. Chapter 2 presents

a review of the anatomy and mechanics of the middle ear. The fundamentals of laser Doppler vibrometry will be reviewed in Chapter 3. Chapter 4 reviews the results of previous studies that are relevant to this one. The methods used in completing this study are discussed in Chapter 5. Chapter 6 presents the results we obtained from studying the linearity, repeatability, inter-animal variability and middle-ear vibration patterns. Conclusions and suggestions for future work are presented in Chapter 7.

CHAPTER 2. Hearing and Anatomy

2.1 Introduction

In this chapter we shall give an overview of hearing physiology followed by a discussion of ear anatomy. The emphasis will be on humans and rats and the differences between these two species.

2.2 Overview of Hearing

2.2.1 Sound

The process of hearing begins with sound. Sound is mechanical radiant energy that is transmitted by longitudinal pressure waves in a material medium and is the objective cause of hearing. The medium is a series of particles, typically air. The source of the wave is typically a vibrating object capable of displacing the particles around it. This vibrating object could be the vocal cords of a human, the string of a guitar or the diaphragm of an audio speaker, for example. The sound is then propagated from one location to another. As one particle is displaced from its equilibrium position it causes the nearest particles to be shifted from their equilibrium positions and this process continues throughout the medium.

2.2.2 Perception

In order for this sound to be perceived, it must be converted into electrical impulses that the brain can interpret. The human ear is shown in Figure 2.1. Hearing starts at the outer ear. The pinna is designed to collect the sound and direct it toward the external auditory canal. The wave travels down the length of the ear canal and strikes the tympanic membrane (eardrum). The tympanic membrane vibrates, sending the vibrations into the middle ear through three small bones called the ossicles. The ossicles send the sound waves to the inner ear and the liquid-filled hearing organ called the cochlea. Here, sound energy is converted to electrical impulses which are sent by the auditory nerve to the brain. The brain then interprets these signals as sound.

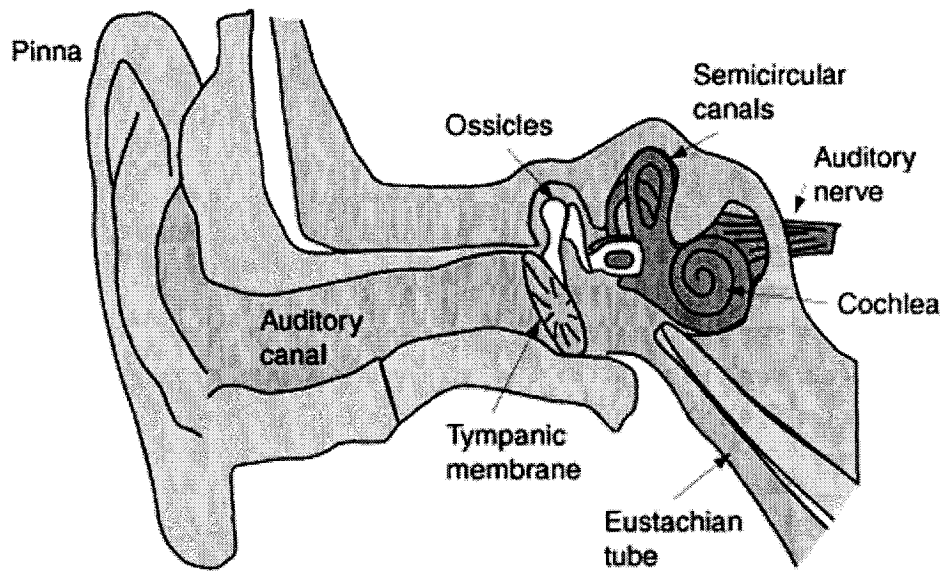


Figure 2. 1 The human ear.
 (<http://hyperphysics.phy-astr.gsu.edu/hbase/sound/ear.html#c3>)

2.2.3 Sound Measurement

The sound pressure at the threshold of pain is about 10 million times larger than the smallest pressure we can perceive. This broad range of intensities that can be detected by the ear can complicate the measurements done in clinical and scientific laboratory settings. Therefore, scientists use the decibel (dB), which compresses the units of measurement to a practical range. The decibel is defined as:

$$\text{Power Difference in dB} = 10 \log_{10} \left[\frac{\text{Power A}}{\text{Power B}} \right]$$

The power of sound varies as the square of pressure. Squaring a value doubles its logarithm. Therefore, the decibel formula for sound pressure becomes:

$$\text{Power Difference in dB} = 20 \log_{10} \left[\frac{\text{Sound Pressure}}{\text{Reference Pressure}} \right]$$

The decibel scale is, therefore, a relative scale comparing sound pressure to a standard reference level. A commonly used reference pressure is $2 \times 10^{-5} \text{ N/m}^2$, a value conventionally taken to represent the smallest sound pressure detectable by humans. Other reference pressures exist, but when $2 \times 10^{-5} \text{ N/m}^2$ is used, sound pressure is denoted as dB SPL (for sound pressure level) (e.g., Templer et al., 1987).

2.3 Temporal Bone

The middle ear and inner ear are located within the temporal bone. The middle ear is a mechanical apparatus and, as such, is sensitive to mechanical disturbances. Many mammalian activities involve vibrations of the skull which would constitute such mechanical disturbances. The simple act of chewing, for example, causes vibrations of the skull.

In most mammals, including humans, the entire hearing organ is integrated into the skull (Figure 2.2b). The middle ear has a bony wall and is fused to the skull, causing the structure to be rigid and immobile relative to the skull. Such an arrangement is only adequate if vibrations of the skull are infrequent and the animal can simply stop the ear-disturbing activity in order to concentrate on the acoustic signal of interest. The rat and many other rodents, for example, gnaw extensively for long periods of time, but can remain alert to acoustic warnings. Isolating the ear from the rest of the skull reduces the mechanical noise caused by such activities (Fleischer, 1978). It has, therefore, been suggested that rodents' ears are partially isolated since they are frequently gnawing. The rodent hearing organ forms a bony capsule which does not incorporate elements of the skull. It is connected to the skull via bridges of cartilage (Figure 2.2a). This setup provides some isolation, especially at higher frequencies (Fleischer, 1978).

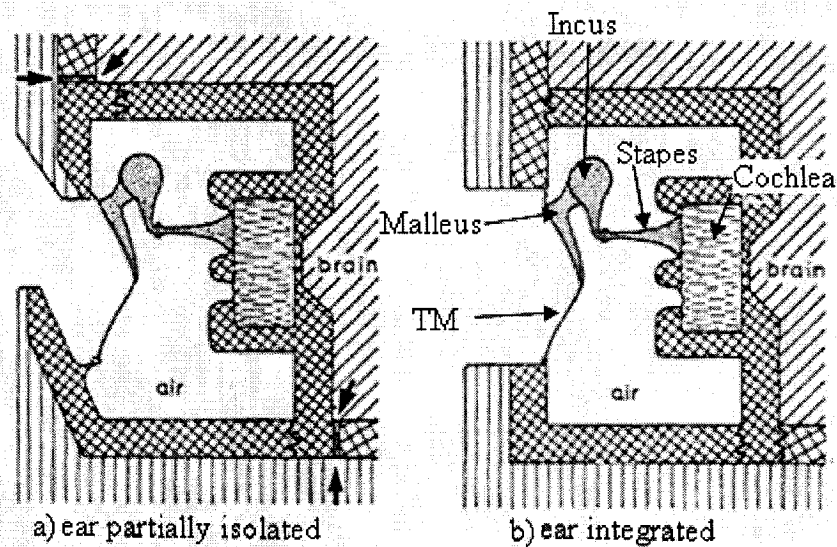


Figure 2. 2 Two different types of ear and skull in terrestrial mammals. Rats have partially isolated (a) middle ears, and humans have integrated (b) middle ears. The black arrows indicate bridges of cartilage. (Modified from Fleischer, 1978)

2.4 Human Middle Ear

2.4.1 Tympanic Membrane

The human tympanic membrane (TM) is roughly conical, pointing inward, and the deepest point is known as the umbo (Figure 2.3). The manubrium of the malleus is attached to the medial side of the TM, and extends down as far as the umbo. The lower part of the tympanic membrane is known as the pars tensa (PT). The pars tensa represents most of the area of the tympanic membrane (Figure 2.4). The fibrous layer of the pars tensa thickens peripherally to form a fibrocartilaginous ring, sometimes referred to as the annulus. This ring anchors the tympanic membrane in a groove known as the tympanic sulcus. The area of the tympanic membrane superior to the lateral process of the malleus is known as the pars flaccida. Both areas of the TM are made up of three layers: squamous epithelium laterally, mucosa medially, and an intermediate fibrous layer. The epidermal layer is continuous with the skin of the external auditory canal, and the mucosal layer is contiguous with the mucous membrane of the middle ear. The fibrous layer of the pars tensa includes a radial and a circular layer. The fibers of the radial layer radiate outward. The fibers of the circular layer are more or less concentric

around the umbo. The fibrous layer of the pars flaccida is less organized. The pars flaccida is usually thicker and more lax than the pars tensa (Vander et al., 1994).

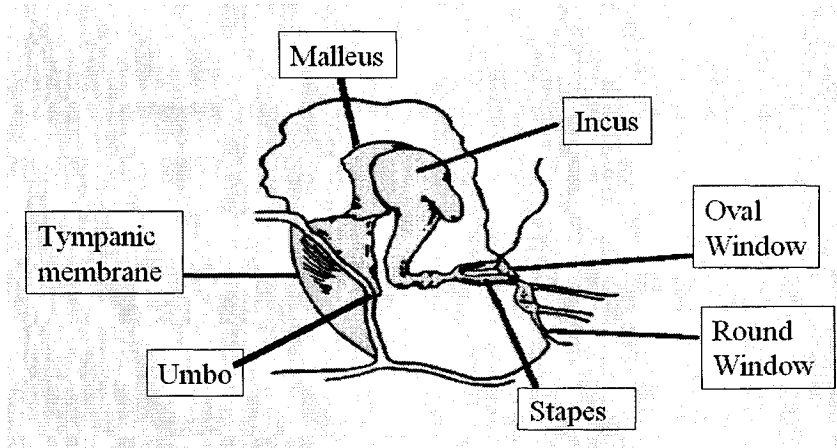


Figure 2.3 The human middle ear. The important structures are labeled.
www.bcm.tmc.edu/oto/studs/anat/tbone.html

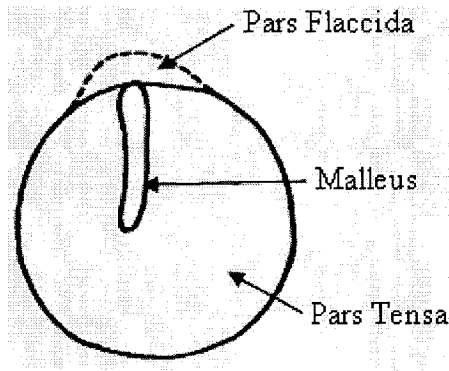


Figure 2.4 Sketch of human tympanic membrane.
(Modified from http://audilab.bmed.mcgill.ca/~funnell/AudiLab/teach/me_saf/me_saf.html)

2.4.2 The Ossicles

A chain of three little bones, called the ossicles, is connected at one end to the tympanic membrane and at the other end to the oval window. This chain consists of the malleus, the incus and the stapes (Figure 2.3). The latter is the smallest bone in the human body (Figure 2.5). The malleus has two processes, a lateral and an anterior one. The malleus connects with the body of the incus. The incus also has two processes, a short one and a long one. The longer one attaches to the stapes through a small piece of bone known as the lenticular process. The stapes consists of an oval-shaped footplate and two crura which merge and connect to the incus at the lenticular process.

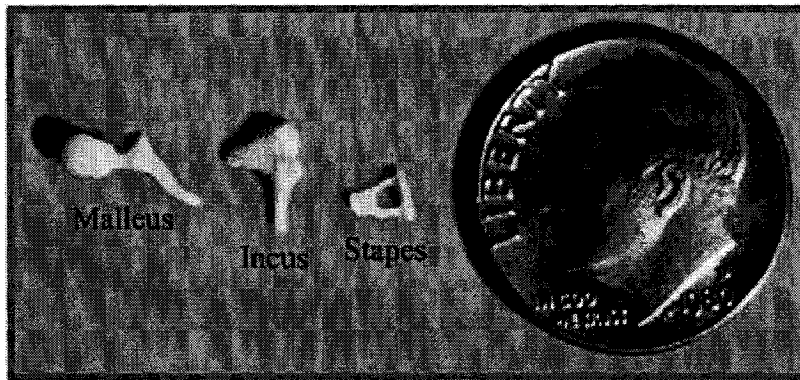


Figure 2.5 The ossicles are compared in size to an American dime.
<http://www.ear-anatomy.com/overview.htm>

2.4.3 The Middle-Ear Muscles

Two small skeletal muscles are found in the middle ear. The tensor tympani attaches to the malleus, and the stapedius attaches to the stapes. There is evidence that these muscles contract reflexively to protect the delicate receptor apparatus of the inner ear from continuous intense sound stimuli and improve hearing over certain frequency ranges. The middle-ear muscles have also been thought to function solely as ligaments, or even to serve no purpose at all for normal hearing (Berge et al., 1990).

2.4.4 The Tympanic Cavity

The middle-ear cavity can be divided into three parts: the hypotympanum, the mesotympanum and the epitympanum. The hypotympanum is the part of the tympanic cavity below the tympanic membrane. The mesotympanum is the area located medial to the tympanic membrane. The epitympanum is the upper portion of the tympanic cavity, above the tympanic membrane. It houses the head of the malleus and the body of the incus (e.g., Templer et al., 1987). The human middle ear also contains a pronounced cell system which extends into the ‘squamous’ portion of the temporal bone. This cell system forms a sponge-like mesh which is filled with air and is in contact with the hypotympanum.

2.5 Rat Middle Ear

The middle ear of the rat contains all the anatomic structures found in the human middle ear. As one might suspect, the ossicles are much smaller in the rat than in humans; they are approximately one quarter as long (Judkins and Li, 1997). The rat’s middle-ear morphology was described by Fleischer (1978) as exhibiting the “microtype” organization. The characteristics of this design are that the malleus is fused to the tympanic ring at the gonial bone and there is a large mass at the head of the malleus called the orbicular apophysis (Figure 2.6).

In humans, the area of the tympanic membrane is approximately 66 mm² (Donaldson et al., 1992), whereas in the rat it is approximately 11 mm² (Zimmer et al., 1994). The relative sizes of the pars tensa and pars flaccida are quite different. Whereas the human has a very small pars flaccida (Figure 2.4) when compared to the total size of the tympanic membrane, in rats the pars flaccida occupies between one quarter and one third of the tympanic membrane area (Figure 2.7).

Instead of the sponge-like cell system found in humans, the rat has a large inferior air space referred to as the bulla (Figure 2.8) (Judkins and Li, 1997).

The rat's greatest hearing sensitivity is at ~40 kHz and it seems to hear up to 100 kHz (Crowley et al., 1965). The greatest sensitivity in humans is between 3 and 4 kHz with the upper limit being ~ 20 kHz in children and ~ 15 kHz in adults.

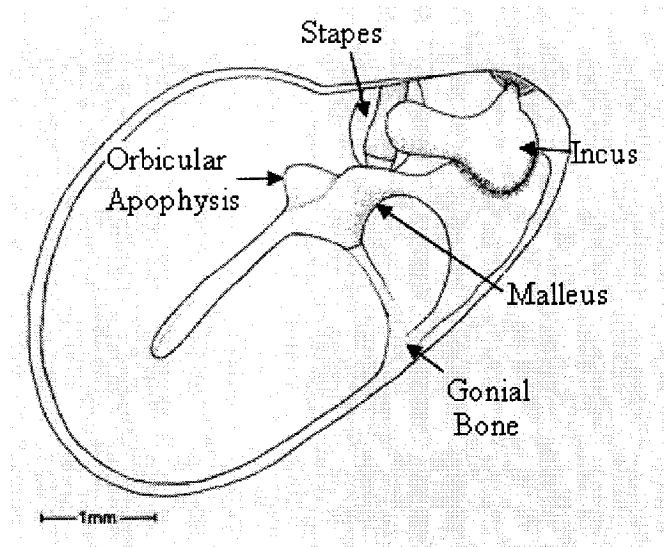


Figure 2. 6 The rat middle ear. Viewed laterally, with tympanic membrane removed. (Modified from Zimmer et al., 1994)

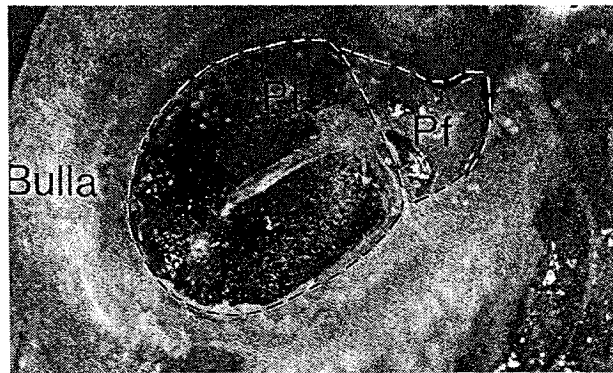


Figure 2. 7 A photomicrograph of the rat tympanic membrane.
The pars tensa (Pt) and pars flaccida (Pf) are shown.
Zimmer et al., 1994

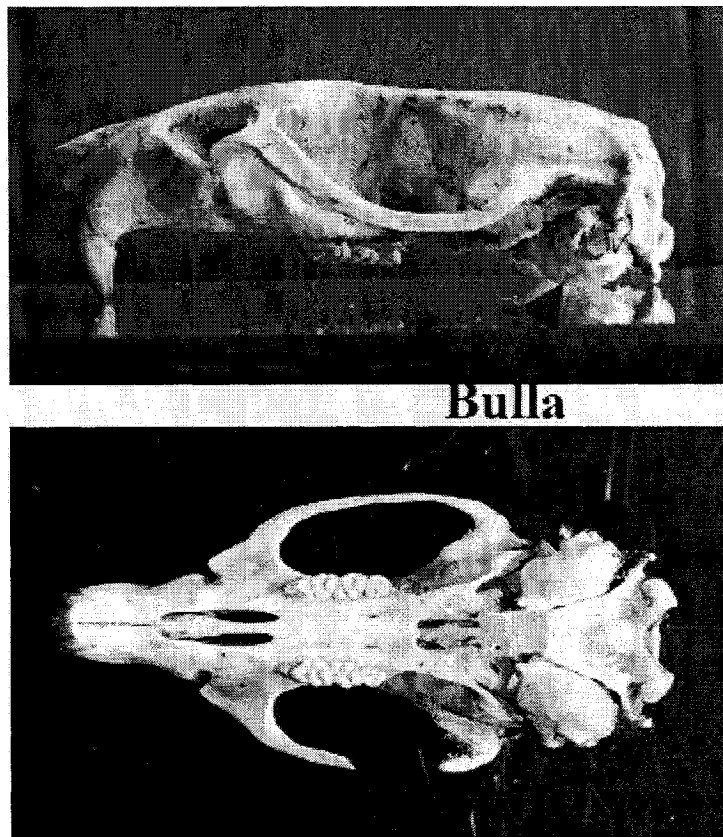


Figure 2. 8 The osseous skull of the rat, photographed from lateral and ventral angles, showing the enlarged air-filled middle-ear bullae.

2.6 Axis of Rotation

In humans, the malleus-incus complex is commonly viewed as having a rotational axis which, at least at low frequencies, runs through two suspensory ligaments: the posterior incudal ligament and the anterior malleolar ligament (Figure 2.9). According to Fleischer (1978), despite the apparent fixation of the malleus in the microtype ear to the tympanic ring, a rotation of the complex is still possible. This connection and the anchoring of the short arm of the incus form a rotational axis similar to that in humans (Figure 2.10). Rats and humans are, however, dissimilar in that the rat manubrium is almost parallel to the axis of rotation, which is not the case in humans (Figure 2.11). Fleischer (1978) also found, through experiments with an enlarged mechanical model, that the additional mass contributed by the presence of the orbicular apophysis shifts the centre of mass of the malleus-incus complex. This adds a second axis of rotation at high frequencies that runs along the transversal part of the malleus (Figure 2.12). He therefore concluded that microtype ears have two axes of rotation and two clearly defined modes of vibration of the malleus (Figure 2.13).

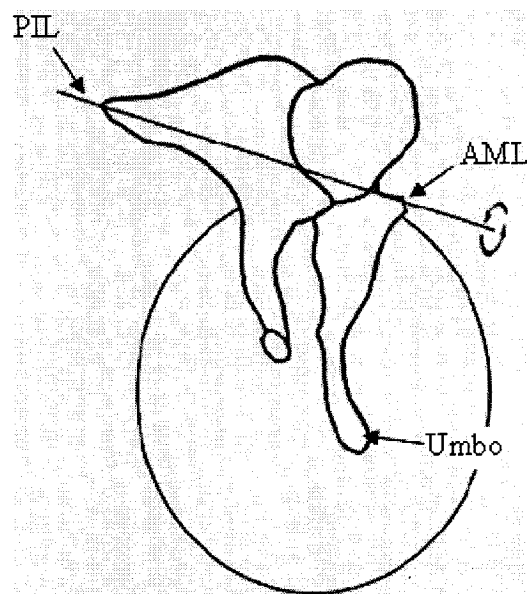


Figure 2. 9 Rotational axis runs through the posterior incudal ligament (PIL) and the anterior malleolar ligament (AML) (Modified from Willi, 2003).

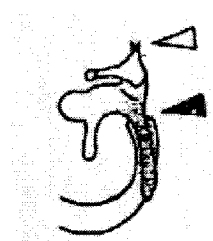


Figure 2. 10 The malleus is fused to the tympanic ring (black arrow) and the incus is anchored (white arrow) giving the microtype ear an axis of rotation similar to that in humans. (Fleischer, 1978)

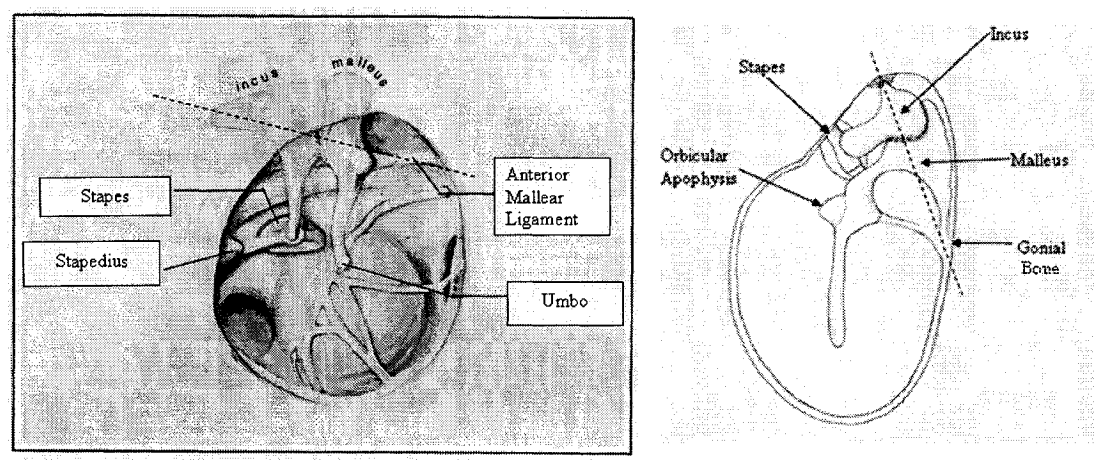


Figure 2. 11 Human (left) and rat (right) middle ears. Viewed from the lateral side, with tympanic membrane removed. Axis of rotation is almost perpendicular to manubrium in humans, but almost parallel in rats. (Left: Modified from Templer et al., 1987; Right: Modified from Zimmer et al., 1994)

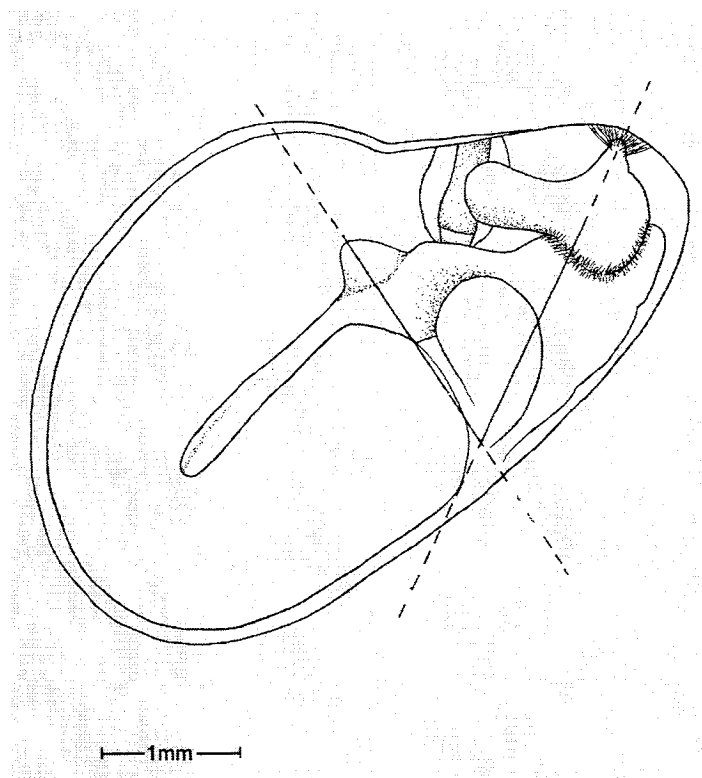


Figure 2. 12 The rat, and other microtypes, have two axes of rotation, as shown here.
 (Modified from Zimmer et al., 1994)

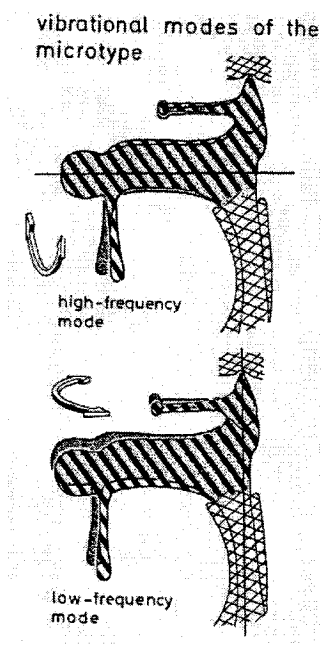


Figure 2. 13 Illustration of the two vibratory modes of the microtype ear.
 (Fleischer, 1978)

2.7 Impedance Matching

The acoustical function of the middle ear is that it serves as an impedance-matching system. Here, impedance is defined as the resistance to the flow of acoustical energy. The ability of a wave to be transferred from one medium to another is dictated by the impedances of the media. When a wave is transferred from air (a low-impedance medium) to liquid (a high-impedance medium), as much as 99.9% of the energy fails to enter the liquid (Feldman and Wilber, 1976). If air-borne sound were to stimulate the liquid-filled cochlea directly, the different impedance characteristics of liquid and air would result in large amounts of energy being lost. The middle ear serves to partially match the impedance of sound in air to the impedance of sound in the cochlea.

The impedance matching of the middle ear is primarily due to the size difference between the tympanic membrane and the oval window. Acoustical pressure in the ear canal acts on the area of the tympanic membrane. As the TM vibrates, the ossicles transmit this movement to the much smaller oval window. Pressure is defined as the force divided by the area over which the force is being applied. If we assume that the force is the same, the pressure applied at the oval window is greater given the smaller surface area over which the force is being applied.

It is commonly assumed that the malleus and incus act together as a mechanical lever system, and that they function in such a way as to provide a mechanical advantage. The fulcrum of this lever system would be one of the axes of rotation discussed earlier. Dividing the distance between the umbo and the rotational axis (M1 and M2 in Figure 2.14) by the distance between the incudo-stapedial joint and the rotation axis (I1 and I2 in Figure 2.14) yields a lever ratio. This lever ratio further increases the force applied at the footplate.

A third mechanism was first presented by Helmholtz (1869, 1877) who suggested that the curvature of the eardrum was an important factor in the impedance matching of

the middle ear. Using a finite-element model, Funnell (1996) showed that a curved tympanic membrane is better able to transfer the forces to the manubrium, thereby increasing the latter's displacements.

The difference in intensity and phase of sound reaching the oval and round windows has been referred to as a fourth mechanism that is believed to contribute to the impedance matching of the middle ear. The round window is an opening in the medial wall of the middle ear; it is covered by a membrane that separates the middle and inner ears. The differences in intensity and phase cause differential displacement of the liquid in the inner ear, producing mechanical stimulation of sensory hair cells (Cummings 2005).

Although all of these mechanisms contribute to the impedance matching of the middle ear, it is not clear how the different mechanisms can be separated (Funnell, 1996).

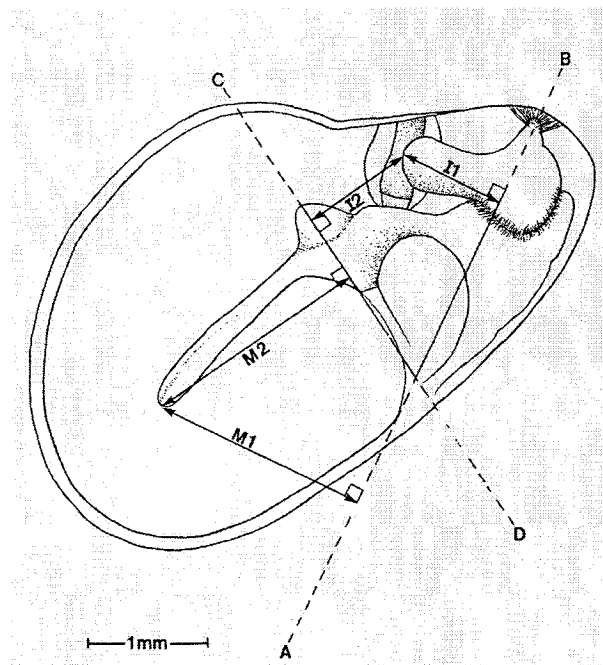


Figure 2. 14 The lever arms for axis of rotation AB are M1 and I1 and for axis CD are M2 and I2. (Modified from Zimmer et al., 1994)

CHAPTER 3. Laser Doppler Vibrometry

3.1 Introduction

Laser Doppler vibrometry provides a reliable method of measuring middle-ear vibration: it is a sensitive non-contacting optical technique that does not load the middle ear and is capable of measuring displacements at the nanometer level (Goode et al., 1993). Furthermore, the large gradual changes in position of middle-ear structures do not affect the accuracy of measurements obtained with this technique.

Section 3.2 will present an introduction to interferometry in general, followed in Section 3.3 by a discussion of heterodyne interferometry, of which laser Doppler vibrometry is one type. The discussion is based in large part on information presented by Hariharan (1992, 2003).

3.2 Interferometry

An interferometer works on the principle that the intensities of two waves that are in phase will reinforce each other, whereas two waves out of phase will tend to cancel each other out.

Optical interferometry works best with a point source of coherent monochromatic light. For many years, a pinhole illuminated by a mercury-vapour lamp was used. This method suffered because the light was not monochromatic, it was only partially coherent and the method did not provide large amounts of light. Coherence means that the variations of the electrical field at any two points in space are completely correlated (Hariharan, 1992).

In light bulbs and fluorescent tubes, the light is incoherent in that it is radiated in random directions at random times. Laser light is monochromatic, coherent and very

directional. Laser stands for **light amplification by stimulated emission of radiation**. A laser is a device that controls the way energized atoms release their photons. It creates and amplifies a narrow, intense beam of coherent light. In 1917, Einstein was the first to point out that “atoms in a higher energy state, which normally radiate spontaneously, could also be stimulated to emit and revert to a lower energy state when irradiated by a wave of the correct frequency.” Schawlow and Townes (1958) first showed that amplification by stimulated emission was possible in the visible region, and that two mirrors could be used to create a simple resonator for mode selection (Hariharan, 2003).

The development of the laser provided an intense source of light with a remarkably high degree of spatial and temporal coherence. Lasers removed most of the limitations imposed by thermal sources and paved the way for many new techniques (Hariharan, 2003).

Several types of lasers exist. The lasing material can be solid, liquid, gas or semiconductor. Gas lasers, such as the helium-neon (He-Ne) lasers used in many vibrometers, have a primary output of visible red light. Helium-neon lasers are commonly used because they are inexpensive and easy to operate. The emission wavelength for helium-neon laser beams is 633 nm (Hariharan, 2003).

3.3 Heterodyne Interferometry

3.3.1 Introduction

When the velocities of interest are very small compared with the velocity of light, the Doppler method cannot be used directly, and heterodyne interferometry is used. This technique involves the use of two beams derived from the same laser with a small frequency shift introduced in one beam of the interferometer (Hariharan, 2003). The velocity of the target is determined by detecting the beats produced by the scattered light and the original laser beam (Hariharan, 2003).

Although heterodyne interferometry allows the measurement of vibration amplitudes of a few thousandths of a nanometer at frequencies above 50 kHz, the accuracy of measurements at lower frequencies suffers due to low-frequency noise (Hariharan, 2003).

Laser Doppler vibrometry is a form of heterodyne interferometry and will be discussed in the following section.

3.3.2 Laser Doppler Vibrometry

Laser Doppler vibrometry (LDV) is based on the Doppler principle. The Doppler effect is the change in the observed frequency of a wave due to relative motion between the source and a fixed point of reference. It is named after the Austrian physicist who was the first to study the phenomenon, in 1842. Frequency changes can occur due to a movement of the source, receiver, propagating medium, or an intervening reflector or scatterer (Drain, 1980). In the case of laser Doppler vibrometry, the shifts are caused by scattering from an object that is moving relative to the light source.

When a wave is reflected by a moving object and detected by a measuring system, such as a laser Doppler vibrometer, the measured frequency shift of the wave is

$$f = \frac{2v}{\lambda},$$

where v is the object's velocity and λ is the wavelength of the in-going wave. Therefore, in order to determine the velocity of an object, one can measure the frequency shift at a known wavelength.

When measuring vibration velocities, one of the beams of the interferometer is reflected from the vibrating object (Figure 3.1). The frequency of the reflected light is shifted by the Doppler effect. Reflection of the beam generates sidebands at frequencies $f_l \pm f_s$, where f_l is the frequency of the beam of light and f_s is the frequency of vibration. This reflected beam is merged with the offset, reference beam. The output from a

photodetector then consists of a component at the offset frequency and two side bands (Hariharan, 2003). The vibration amplitude a can then be calculated from the relation

$$\frac{2\pi a}{\lambda} = \frac{I_s}{I_o},$$

where I_o is the power at the offset frequency and I_s is the power in each of the sidebands (Hariharan, 1992).

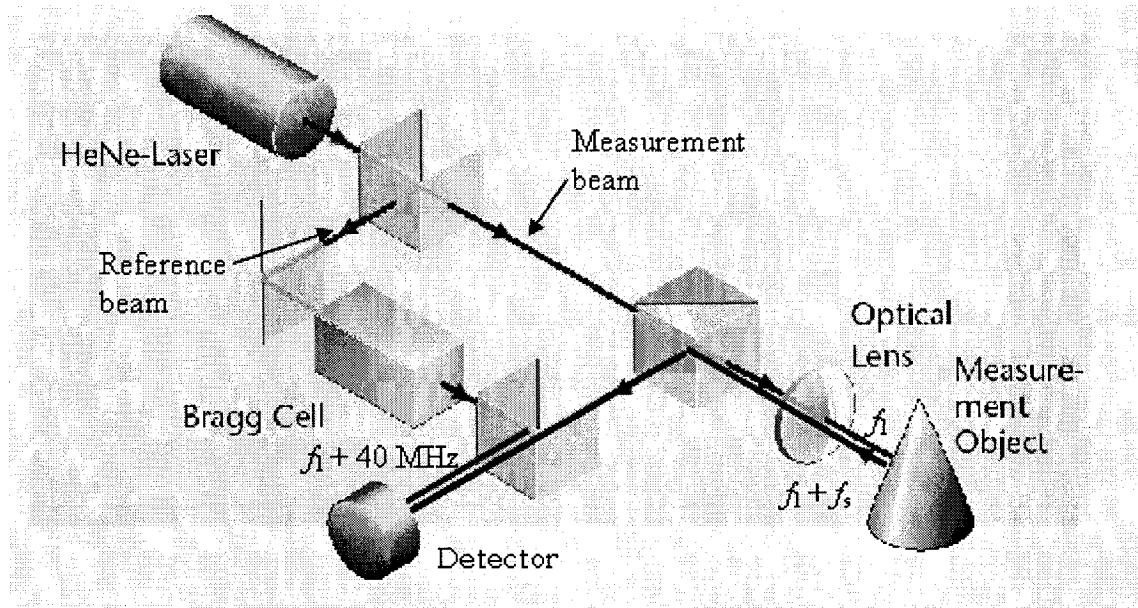


Figure 3. 1 A beam of laser light is split into a reference beam and a measurement beam. The measurement beam is focused onto the object of interest and reflected back. The reflected beam is then merged with the reference beam after it has been offset by the Bragg cell, and the combined beams are sent to a detector.

(Modified from www.polytec.com/usa/158_463.asp?highlightSubMenu=Vibrometer%20University)

It is important to know the direction of motion of vibrating surfaces. Laser Doppler vibrometers make use of an acousto-optic modulator, also known as a Bragg cell, to help determine the direction the object is moving in. A typical modulator consists of a glass block with a piezoelectric transducer bonded to it. It shifts the light frequency by 40 MHz (Mayinger and Feldmann, 2001). A stationary object therefore results in a 40 MHz modulation frequency of the fringe pattern. When the object moves towards the interferometer, the modulation frequency is reduced, and when it moves away the frequency is greater.

3.4 Conclusion

Laser Doppler vibrometry provides a simple, accurate method of measuring middle-ear vibrations. It is capable of measuring nanometer levels of displacements without contacting or loading the vibrating structure.

Laser Doppler vibrometry has been used for several animal, temporal-bone and live-human studies. Studies by Huber et al. (2001) and Rosowski et al. (2003) have shown possible diagnostic uses for this technology. LDV measurements were shown to differentiate normal ears from diseased ones in some cases where standard audiological tests failed.

CHAPTER 4. Previous Studies

4.1 Introduction

Our present research involves the *post mortem* study of tympanic-membrane vibrations of rats. In this chapter we shall outline previous studies that are important in understanding this research. Section 4.2 will discuss the validity of using *post mortem* middle ears as opposed to live ones. Section 4.3 goes over the findings of past rat studies. Section 4.4 discusses a study done on mice, which also have the microtype middle ears described by Fleischer (1978). Section 4.5 contains a brief summary of studies done to describe the motion of the malleus.

4.2 *Post Mortem* Middle Ear

Several studies have shown that the middle ear can remain relatively normal for hours, or even days, after death if special steps are taken to maintain the normal behaviour. Rosowski (1990) measured the input impedance in fresh and thawed human temporal bones and compared the measurements with *in vivo* data obtained with similar instruments. His measurements of *post mortem* middle ears compared well with the normal ranges for living ears. Measurements reported by Rosowski (1990) in guinea pigs and by Khanna and Tonndorf (1972) in the cat also suggest that the *post mortem* middle ear functions similarly to that of a live subject. Goode et al. (1993, 1996) compared umbo-motion measurements made by themselves and others on cadavers with those made on live ears. In 1993, they concluded that the acoustic properties of the TM were no different in live human ears and temporal bone models at low and mid frequencies. In 1996 they compared their own averaged results and showed that no significant differences exist below 6000 Hz (Figure 4.1).

Ruggero and Temchin (2003) argued, based on comparisons of *post mortem* and *in vivo* studies of umbo and stapes vibrations, that there are important differences

between living and *post mortem* middle ears. Although there was only one *in vivo* measurement of stapes vibrations, they compared three *in vivo* umbo measurements with four *post mortem* responses. Their results were normalized to the velocity at 1 kHz and plotted on a decibel scale against frequency (Figure 4.2). They argued that whereas *in vivo* responses were relatively flat over wide ranges, “*postmortem* responses vary widely above 2 kHz.” Rosowski et al. (2004) later argued the opposite, attributing the differences observed by Ruggero and Temchin (2003) to differences in measurement techniques, the state of the middle ear cavity, middle-ear muscle tone and the loss of active mechanisms in the cochlea. Rosowski et al. (2004) found that the live-ear studies generally fell within the 95% confidence interval around the grouped temporal-bone results (Figure 4.3).

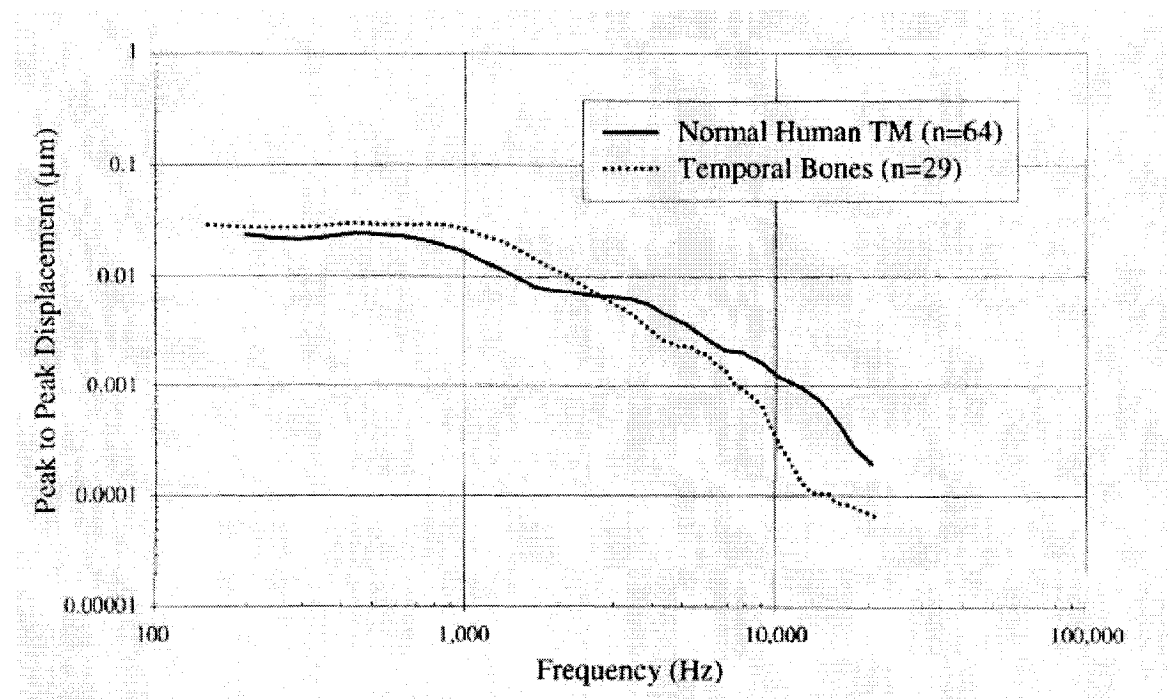


Figure 4. 1 Goode et al. concluded that there were no significant differences between live human and temporal bone models below 6 000 Hz. (Goode et al., 1996)

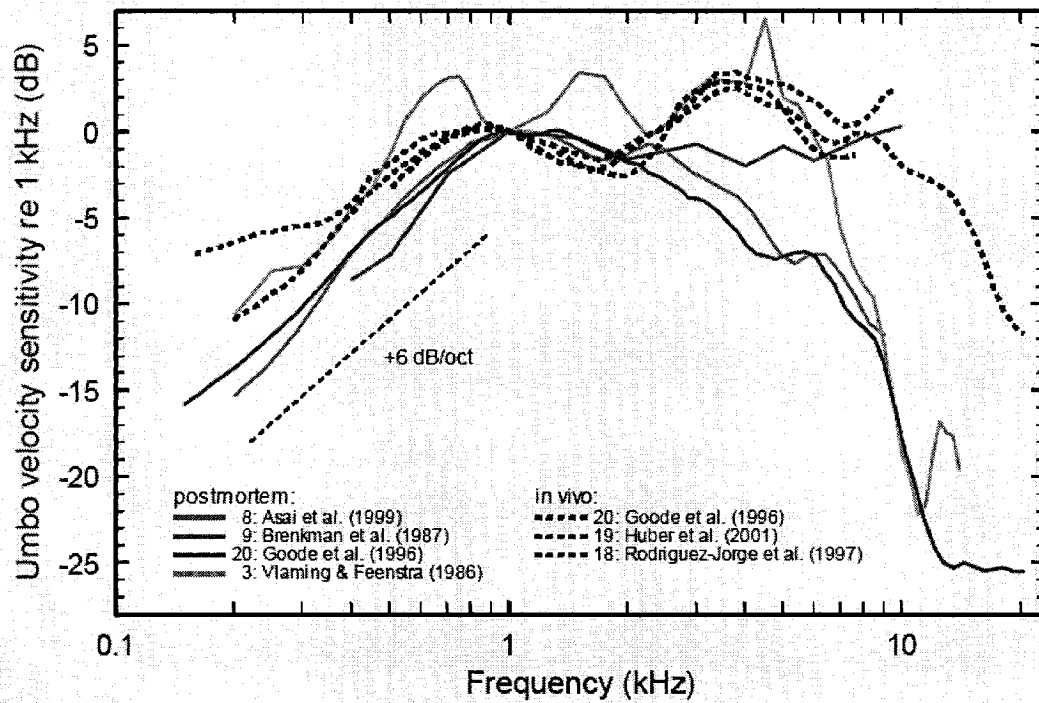


Figure 4. 2 Umbo frequency responses have been normalized to 1 kHz. *In vivo* results are flatter over a wider range than the *post mortem* ones. (Ruggero and Temchin, 2003)

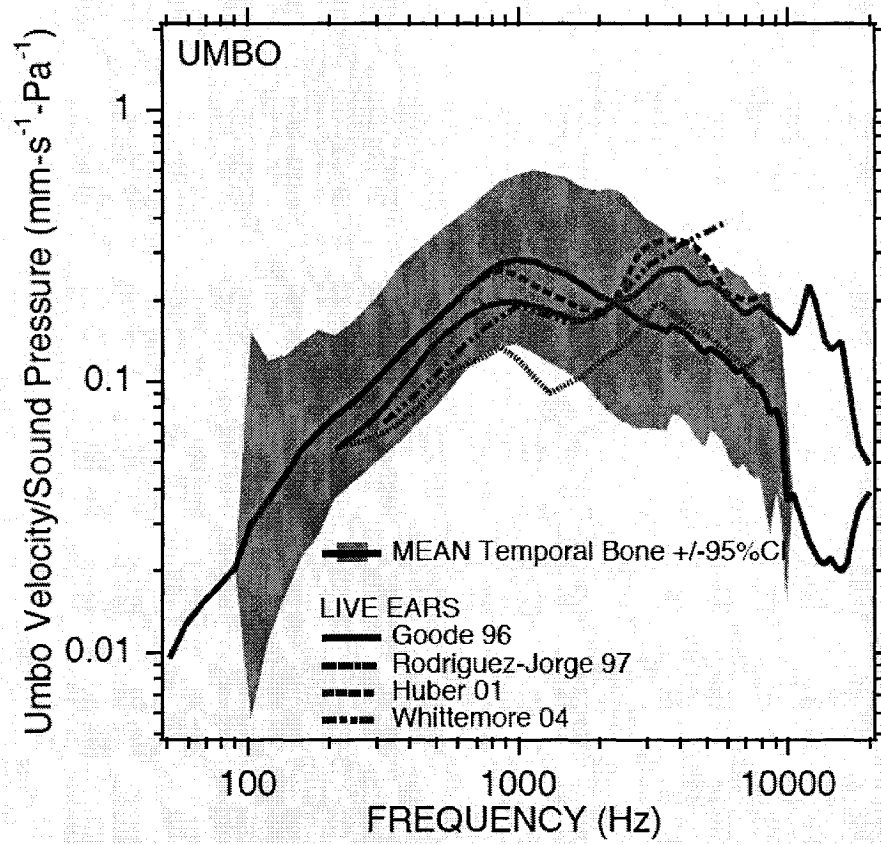


Figure 4.3 Comparison of the mean and 95% confidence intervals of *post mortem* ears to the means of four *in vivo* frequency responses. (Rosowski et al., 2004)

4.3 Rat Studies

Few measurements have been made in the past to study the rat's middle ear. Early studies by Beccari and Molinengo (1958) and by Ishii et al. (1964) reported the frequencies of maximum sensitivity of the ear, but no frequency responses were shown. Ishii et al. (1964) studied the characteristics of rat hearing using cochlear microphonics. Although they were studying the teratogenic effects of auditory stimulation and did not investigate middle-ear mechanics explicitly, some relevant findings were reported. They determined that the upper limit of the audible range of the rat was 100 000 Hz, and, although an exact lower limit was not obtained, their results indicate that rats can hear sounds at frequencies below 300 Hz. Sensitivity of the rat ear was found to be high at about 1 500, 7 000 – 7 500, and 15 000 Hz (Ishii et al., 1964; Beccari and Molinengo, 1958).

Doan et al. (1996) reported a study on the development of the rat middle ear. The tympanic membrane was stimulated with pure-tone sounds and the motion of the umbo was measured using a laser interferometer. Velocity responses were obtained as a function of age, sound intensity and frequency. They found that umbo velocity responded linearly with respect to sound intensity at least above 90 dB SPL. The apparent nonlinearities at the lower sound pressure levels were attributed to noise in the laser signal and not to nonlinearities in the umbo velocity. Tympanic-membrane velocity was also shown to increase as the pups aged. The magnitude and pattern of the rise in velocity were not consistent, but results showed that the middle ear reached threshold values for all measured frequencies by 68 days after birth. Although the results were quite variable, the velocity responses from five adult rats showed three characteristic peaks at about 2.3, 6.3 and 20.0 kHz.

When studying the effect of tympanic membrane perforation size on umbo velocity in the rat, Bigelow et al. (1996) reported the frequency response of the intact tympanic membrane as a control. Laser interferometry was used to measure umbo velocities when the tympanic membrane was stimulated with pure-tone sounds at

frequencies between 1.0 and 40 kHz. Velocity responses from five rats were averaged and presented. They found three peaks in the averaged velocity response, at about 2.5, 5.5, and 15.0 kHz. These peaks were described as representing the contributions of unique structural interactions within the middle-ear system.

In a later study, Bigelow et al. (1998) examined the effects of healed tympanic membrane perforations on umbo velocity. Laser interferometry was again used to measure the tympanic membrane velocity at the umbo, and pure-tone stimuli were again presented at frequencies between 1.0 and 40.0 kHz. The frequency responses from eight rats were averaged and presented. The three peaks in the averaged velocity response of the control rats were at approximately 1.5, 5.0 and 14 kHz.

Table 4.1 summarizes the findings of the previous studies for the frequency range we are measuring.

Study	Low-Frequency Sensitivity	High-Frequency Sensitivity
Beccari and Molinengo, 1958 Ishii et al., 1964	1.5 kHz	7.0 – 7.5 kHz
Doan et al., 1996	2.3 kHz	6.3 kHz
Bigelow et al., 1996	2.5 kHz	5.5 kHz
Bigelow et al., 1998	1.5 kHz	5.0 kHz

Table 4.1 Middle ear sensitivity of rats as measured in previous studies.

4.4 Microtype Study

Fleischer's (1978) theory that the orbicular apophysis results in two axes of rotation in microtype ears (cf. Section 2.4) was based on the movements of an enlarged mechanical model. Animal studies had not been performed to validate his theory at that time. Saunders and Summers (1982) did investigate the microtype ear in the mouse. They used a capacitive probe to measure the displacement and velocity responses for test frequencies between 1.5 and 35.0 kHz. Measurements were done at the umbo, the transverse portion of the malleus, and the head of the incus. Umbo measurements at varying sound pressure levels demonstrated the linearity of the tympanic membrane response. Differences in the high-frequency velocity response between the umbo and the transverse process of the malleus were consistent with the shift in rotational axis predicted by Fleischer (1978). Saunders and Summers (1982) concluded that the velocity difference increased rapidly above 4 kHz (Figure 4.4b). However, they reported significant differences between locations only above 18.0 kHz (Figure 4.4a).

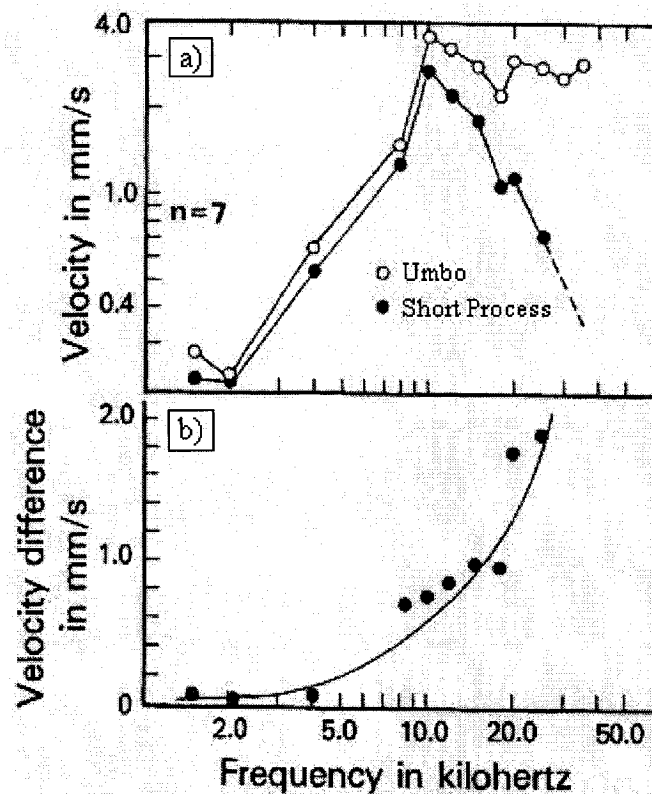


Figure 4.4 Velocity responses of the mouse middle ear at the umbo and short process (a), and velocity differences between these points (b) show an increase in relative velocity between these two points at higher frequencies. (Modified from Saunders and Summers, 1982)

4.5 Motion of the Malleus

Previous studies have used several different techniques to measure displacements at the umbo. The capacitive probe was used by Békésy (1960), Wever and Lawrence (1954), Relkin and Saunders (1980), and Saunders and Summers (1982). Guinan and Peake (1967) employed stroboscopic illumination for their research. The Mössbauer method was used by Gilad et al. (1967), Gummer et al. (1989), and Ruggero et al. (1990). Buunen and Vlaming (1981) used laser Doppler velocimetry. Tonndorf and Khanna (1967), Decraemer et al. (1989, 1990, 1994), Decraemer and Khanna (1994) and many others made use of laser interferometry in their study. Time-average holography was used by Khanna (1970), Khanna and Tonndorf (1972), and Tonndorf and Khanna (1972). In all of the above-mentioned studies, except for one of the studies by Decraemer et al.

(1994), only the motion component along a single observation direction was measured. In order for single component measurements to be valid, one would have to assume that points on the manubrium vibrate only, or mainly, along the “direction of motion,” implying that the manubrium rotates about a fixed axis.

Using heterodyne interferometry to obtain very precise measurements of the motion of the manubrium in cats, Decraemer et al. (1991) showed that the manubrium does not, in fact, move as a rigid body rotating about a fixed axis. Their results showed evidence that the axis of rotation was not fixed and suggested that the manubrium bends at higher frequencies. Funnell et al. (1992) then used a finite-element model to show that manubrial bending is to be expected on theoretical grounds. Decraemer and Khanna (1994) again showed that the motion of the malleus in the cat is quite complex and dependent on frequency. The data showed that malleus motion is a frequency-dependent combination of translation and rotation. By measuring the three-dimensional vibrations of a single point on the umbo, it was shown that the tip of the manubrium did not vibrate in a straight line, but seemed to be following an elliptical path (Decraemer et al., 1994). The shape and inclination of the ellipse with respect to the malleus changed with frequency, supporting the earlier findings that the mode of malleus vibration changes with frequency (Decraemer and Khanna, 1994).

4.6 Conclusions

We believe there is enough evidence supporting the use of *post mortem* middle ears and showing that the *post mortem* measurements will be indicative of *in vivo* behaviour based on the studies presented above.

The results from the few studies dealing with the mechanics of the rat middle ear will serve as an important point of comparison for the measurements reported here. Saunders and Summers' (1982) study of mouse middle-ear mechanics is also important since we will also be dealing with the microtype organization in the rat middle ear.

Although studies investigating the three-dimensional motion of the rat's manubrium have yet to be done, we cannot assume that the malleus vibrates rigidly or along a fixed axis of rotation based on the discussion of Section 4.5.

CHAPTER 5. Methodology

5.1 Introduction

This chapter will describe the methods involved in obtaining our experimental results. The protocol followed in preparing the specimens is outlined in Section 5.2. Sections 5.3 and 5.4 describe the acoustical and optical systems used in our experiments. A brief discussion on the fundamentals of signal analysis is given in Section 5.5. Section 5.6 presents the various issues we investigated, the results of which are presented in Chapter 6.

5.2 Specimen Preparation

Measurements were carried out on seven Sprague Dawley rats supplied by Charles-River (St-Constant, QC). All data were obtained within three hours of the time of death. Table 7.1 provides details about the rats used in this study. The left ear was used in each case for consistency.

	Sex	Age (months)	Weight (g)	No. points
Rat #1	Male	5	620	7
Rat #2	Female	3	380	7
Rat #3	Female	3	390	7
Rat #4	Male	3	473	3
Rat #5	Male	3	410	3
Rat #6	Male	3	387	3
Rat #7	Female	3	222	3

Table 5. 1 Table showing details of the rats used. The “No. points” column refers to the number of points at which frequency responses were measured in each animal.

After the rats were sacrificed, the head was removed from the rest of the body to facilitate the dissection. The lower jaw was removed to completely expose the bulla.

The external ear was removed up to the cartilaginous part of the ear canal and parts of the bony ear-canal wall were removed with a drill to optimize exposure to the tympanic membrane and manubrium. During the dissections, the area of interest was kept moist by constant application of saline solution. This was done to prevent drying out of the tympanic membrane and middle-ear structures. Once measurements were started, no more solution was applied to the middle ear. The area was sealed with Plasticine™ in order to avoid drying of the middle-ear structures.

The air pressure needs to be the same on both sides of the tympanic membrane for it to vibrate normally. When the air pressure within the middle ear is less than that of the external environment, the TM is sucked in. If the air pressure within the middle ear is greater than the external pressure, this causes the TM to balloon outwards. Both situations reduce the mobility of the eardrum. The middle-ear pressure is usually equilibrated with the atmosphere through the opening of the Eustachian tube, which connects the middle ear to the nasopharynx (e.g., Vander et al., 1994). Since the experiments performed here were *post mortem*, the animal cannot equilibrate the middle-ear pressure. Therefore, a small hole was drilled into the bulla, equalizing the pressures on the two sides of the TM. This hole was then covered with Plasticine™ in order to minimize any effects on the acoustical properties of the bulla.

5.3 Acoustical System

It is important that the stimulus is presented and monitored in a way that does not impede the laser beam coming from the vibrometer. An ER-2 TubePhone™ (Etymotic Research) was used as the sound-delivery system, and the sound-pressure level was monitored with an ER-7C (Etymotic Research) probe-microphone system (Figure 5.1a). The sound-delivery and probe-microphone tubes were inserted into a 0.5-cc cylindrical sound chamber, sealed at the top with a glass cover slip. The sound chamber was constructed from a hollow plastic cylinder (the body of a 3-cc syringe) that was cut to the desired length and had two small holes drilled into it. The tubes supplied with the sound-delivery and probe-microphone systems were inserted into these holes (Figure 5.1b). The

tip of the probe-microphone system tube was placed 2–3 mm from the tympanic membrane. The sound chamber was held in place on the skull with Plasticine™. It was placed above the auditory canal, and the surrounding region was also sealed with Plasticine™ to prevent drying and sound loss. The setup is shown in Figure 5.2.

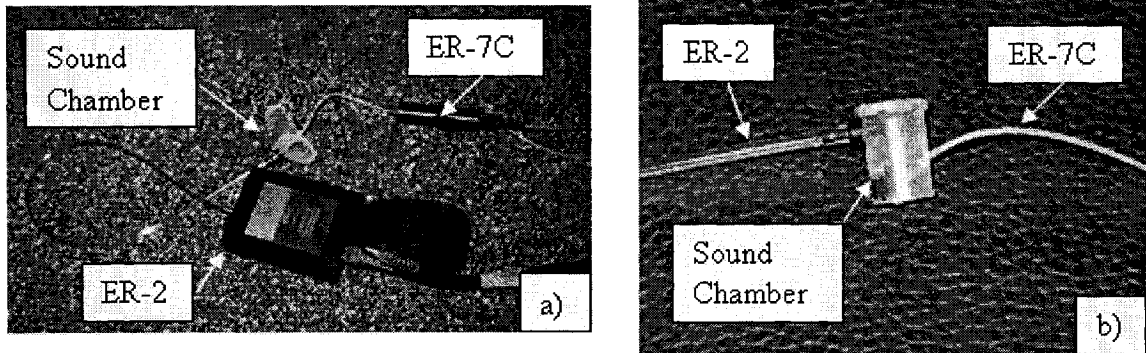


Figure 5. 1 The tubes from the ER-2 sound-delivery system and the ER-7C probe-microphone system fit into two holes drilled into the sound chamber.

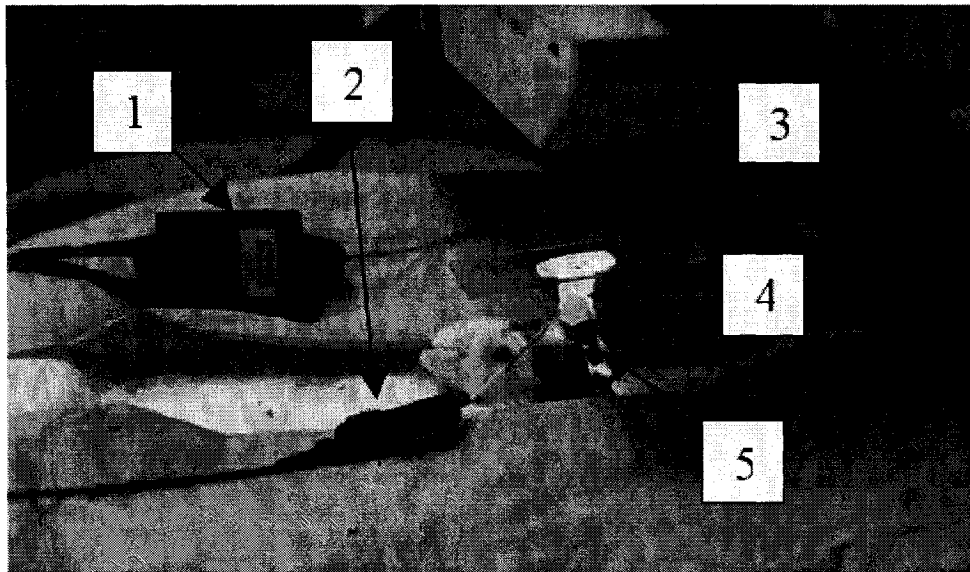


Figure 5. 2 Photograph of experimental setup. 1 = ER-2 Tubeophone™, 2 = ER-7C probe microphone system, 3 = glass cover slip, 4 = sound chamber, 5 = Plasticine™

Measurements were done within a C-14 model double-walled audiometric sound room (Génie Audio, St-Laurent, QC) (Figure 5.3) to attenuate any outside noise that might compromise the measured frequency responses. The dimensions of the C-14 model we used are shown in Table 5.2 and the acoustic performance attenuation graph as supplied by the manufacturer is shown in Figure 5.4.

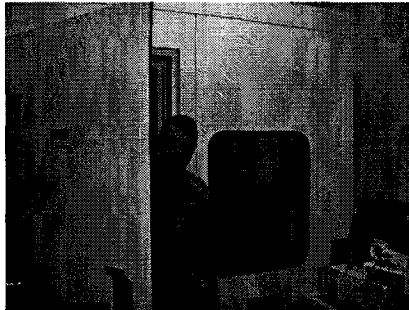


Figure 5.3 Measurements were done within a double-walled audiometric sound room.

<i>Model</i>	<i>Inside Dim.</i>	<i>Outside Dim.</i>
C-14	66" x 77" x 78" 1676 x 1956 x 1981 mm	74" x 85" x 95" 1880 x 2159 x 2413 mm

Table 5.2 Inside and outside dimensions of the C-14 audiometric sound room as supplied by Génie Audio.

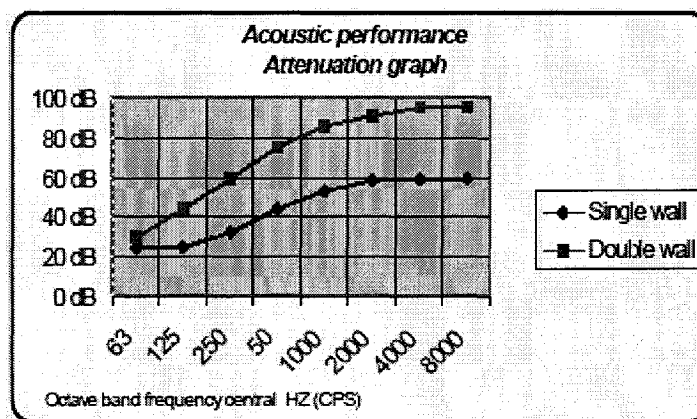


Figure 5.4 Acoustic performance attenuation graph supplied by Génie Audio.

The frequency range studied is limited by the acoustical system being used. The ER-7C probe-microphone system is designed to be flat past 10 kHz. Its limits are ± 2.5 dB between 0.25 and 10 kHz (Figure 5.5). The ER-2 Tubephone sound-delivery system is useful only up to approximately 10 kHz, as can be seen in Figure 5.6. The tests were performed by the manufacturer on a Zwislocki coupler, which is an acoustic ear simulator.

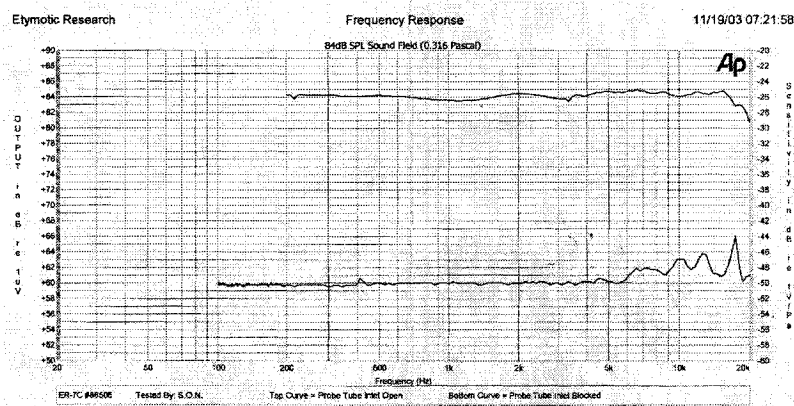


Figure 5. 5 Typical Frequency response of the ER-7C probe-microphone system as provided by Etymotic Research.

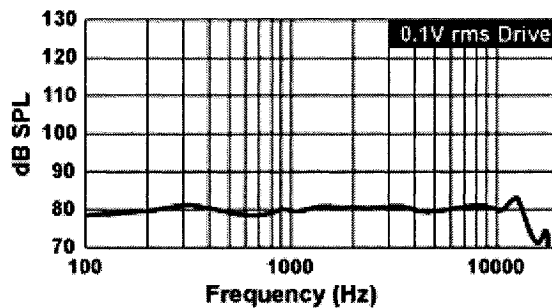


Figure 5. 6 Typical frequency response of the ER-2 sound delivery system.
(<http://www.etymotic.com/pro/er2-ts.asp>)

5.4 Optical System

Displacements were measured using a laser Doppler system (Polytec HLV 1000) coupled to an operating microscope (Zeiss, OPMI-1). Polytec developed the HLV-1000 Hearing Laser Vibrometer specifically for measuring frequency responses in the middle ear and in hearing devices. The system consists of a compact laser Doppler vibrometer (LDV) with a head that mounts to an operating microscope (Figure 5.7); an excitation source; and a complete data acquisition and analysis system. The system includes a computer with a 1.9-GHz AMD processor, 512 MB of RAM and 80 GB of hard-disk space. The software used for processing the data is VibSoft 4.1. The vibrometer is capable of measuring vibrations up to the 30 MHz range with very linear phase response and high accuracy. Low-frequency noise is a problem when using this technique, however, due to the inherently low velocities at low vibration frequencies (cf. Section 3.3.1).

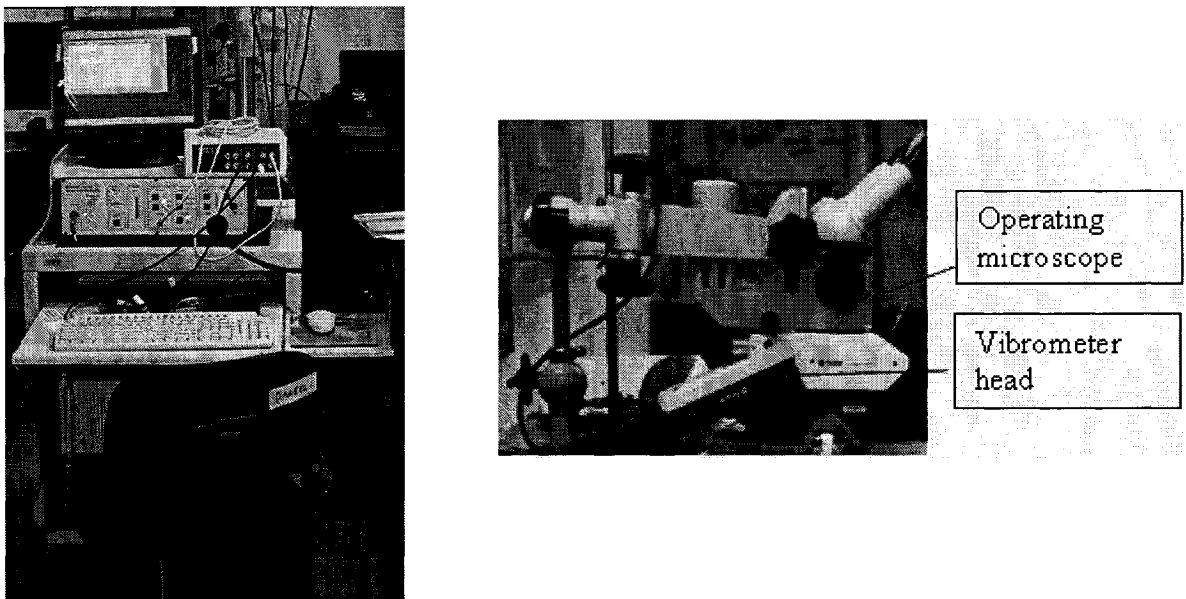


Figure 5.7 *Left:* HLV-1000 vibrometer system. *Right:* The head of the vibrometer mounts to an operating microscope.

The signal-to-noise ratio of laser vibrometer measurements is affected by the amount of backscattered light, which is low for biological tissues, requiring a method of increasing reflectivity. Biological tissues have high anisotropy coefficients, between 0.9

and 0.99 (Vogel et al., 1997). Here, anisotropy coefficients are a measure of the amount of light that will be lost to forward scattering and do not refer to the variation of material properties with the orientation of the tissue. A coefficient of one indicates complete scattering of light. The high value for this coefficient in biological tissues suggests that much light will be lost to forward scattering. Additional light is lost because the plane of the tympanic membrane is not normal to the direction of the incident beam. These phenomena were compensated for in this work by placement of hollow glass micro beads (90 – 150 μm in diameter, Sigma) on the tympanic membrane. These beads act as retroreflectors, returning a large portion of the light in the direction of the incident beam.

The micro beads were held in place by simple capillary force provided by the moisture of the tympanic membrane. It is important that the bead follow the vibrations of the underlying membrane. Decraemer et al. (1989) measured the frequency response of a bead placed on the tip of the manubrium and of a naturally bright reflective spot on the malleus, adjacent to the bead. A comparison of the two responses showed that the ratio of the two amplitudes remained between 0.85 and 1.15, and the phase difference remained between -10° and $+25^\circ$, between 130 and 25 000 Hz. The amplitude and phase differences across the frequency range we used (1 000 to 10 000 Hz) were even smaller, limited to between 0.9 and 1.1 for the amplitude and -5° and $+10^\circ$ for the phase. This close agreement shows that the bead followed the vibrations of the underlying structure very closely, increasing signal-to-noise ratio greatly without much effect on the frequency response.

5.5 Signal Analysis

This section deals with the fundamentals of signal analysis. Fourier's theorem will be presented followed by a discussion of digitization. Methods used to analyze the data more effectively, such as overlapping and windowing, are also presented. The following discussion is largely based on information from Agilent (2002).

In 1807, Joseph Fourier showed that any periodic function can be described as a sum of sine and/or cosine functions. A Fourier series is represented by the infinite sum

$$F(t) = \sum_{i=1}^{\infty} (a_i \sin i\omega t + b_i \cos i\omega t),$$

where $\omega = 2\pi f = \frac{2\pi}{T}$. The function has thus been described as a sum of harmonic components whose frequencies are integer multiples of f , the frequency of the periodic function. a_i and b_i are the Fourier coefficients and indicate the amplitude of the i th harmonic function. The Fourier transformation decomposes any time signal into a sum of vibrations with different frequencies. Decomposing the signal does not add or remove any information if an infinite number of terms is used. The original time signal can be obtained with an inverse transformation.

The data in the time domain comprise a record of the change of a system as a function of time. An actual analog time signal consists of an infinite number of samples with an infinitely short sampling period. To convert an analog signal into a digital one, it must be sampled. The resulting limited number of samples and the finite number of bits per sample result in a loss of information. In order for the digital samples to accurately provide the same information as the analog signal, the sampling frequency must be more than two times the maximum signal frequency.

The data in the time domain are split into blocks of N consecutive, equally spaced samples of the input. These time-domain samples are transformed into $N/2$ equally spaced samples in the frequency domain. There is half the number of samples because each frequency sample contains two pieces of information, the amplitude and the phase. The blocks of time samples lines can be overlapped in order to evaluate changes in the data more effectively. With an overlap of zero, the blocks are right next to each other, and with a value larger than zero, the blocks overlap by that amount.

Since the frequency-domain data are discrete, only data from frequencies which fall on one of the frequency lines are shown correctly. The information from frequencies

that do not fall on a frequency line is distributed over existing lines. This effect can be reduced by applying window functions. Window functions work by setting a value of zero at the beginning and end of the time window, thus avoiding signal jumps at the edges of the time window. There are many windowing functions, but perhaps the most common one is the Hanning window. Hanning windows have the shape of an inverse, lifted cosine function (Figure 5.8). It can, therefore, attenuate information that might be spread widely through the spectrum. In order to use all the data in the time record equally or uniformly, the rectangular window should be used (Figure 5.9). The rectangular window simply cuts off the time signal outside the time window. Rectangular windows can cause high-frequency components if the signal is not equal to zero at the start and finish of the time window. Windows like the Hanning reduce this effect.

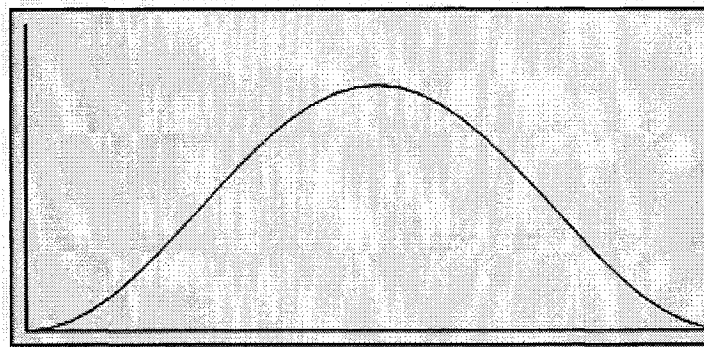


Figure 5.8 Hanning window.

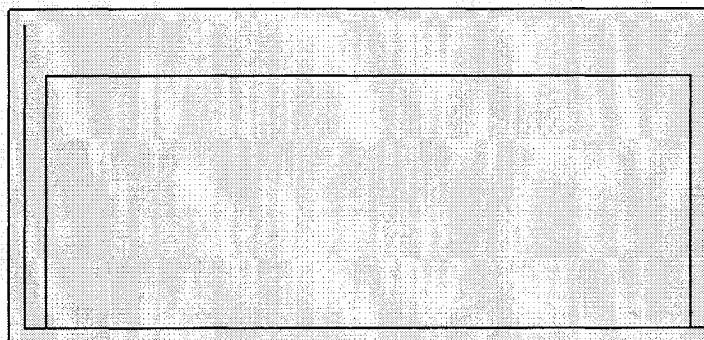


Figure 5.9 Rectangular window.

5.6 Investigations

5.6.1 Excitation Signal

When making a vibrational analysis, it is important to choose the appropriate excitation signal. Not only does the quality of the measurement depend on the stimulus, but the purpose of the measurement should dictate the choice of excitation signal. In the case of an analysis of the displacement patterns of the natural modes of vibration, for example, a complete spectrum must be measured. However, if one is more interested in finding the maximum displacement on a structure, it may be sufficient to measure the deflection shapes at the dominant resonance frequencies. Also important are the signal-to-noise ratio and sampling time. There is often a trade-off between these two criteria (Schüssler and Wörtge, 1998).

Sinusoidal excitation is used to measure the deflection at one particular frequency. The entire time window is dedicated to one frequency and the result is a very good signal-to-noise ratio. If one is interested in studying a complete spectrum, however, obtaining a high frequency resolution is extremely time-consuming.

Swept sine signals “sweep” through the frequencies in the range of interest. Using this method allows the investigation of a broad spectrum at a high frequency resolution in a short amount of time. Although the signal-to-noise ratio suffers, averaging the results provides a way of eliminating noise. The length of the time sample is dependent on the bandwidth and number of frequency lines selected. Dividing the bandwidth by the number of lines yields the resolution in the frequency domain, the inverse of which gives the sample time.

In order to show that the swept signal is reliable and yields accurate results, measurements were taken at the same point using pure-tone sinusoidal excitation and sweep-signal excitation. An animal was prepared as described earlier and measurements were taken on the short process of the malleus. Despite the placement of the reflective beads, the strength of the signal tends to fluctuate. In this particular animal, the signal at the short process was strong and consistent. Given the large number of measurements

required, and the amount of time involved in acquiring all the measurements, the short process provided a good choice of location. First a signal sweeping from 250 – 10 000 Hz was applied and the frequency response was measured. Then 45 pure-tone signals were presented ranging in frequency from 1 000 – 10 000 Hz. Since the pure-tone measurements take a long time to complete, another measurement was taken using the sweeping signal as the stimulus to ensure that any discrepancies between the two stimuli would not be a result of system changes due to time. The 45 pure-tone measurements took approximately 30 minutes to obtain. Each sweep response took approximately 1 min to acquire after being averaged 30 times. The results are shown in Section 6.2.

5.6.2 Noise Floor

In order to establish the lower limit of vibration measurement, a measure of the noise floor is needed, i.e., the amount of displacement measured in the absence of a stimulus. A plot of short-process displacements as well as the noise floor will be presented in Section 6.3 and will indicate the range of frequencies for which we can accurately measure displacements.

5.6.3 Linearity

Input/output testing is a very powerful tool when a system behaves linearly. When a system responds to one input by outputting a value a and another input results in a value b , the output of a linear system in response to both inputs simultaneously would be $a+b$. No real system is completely linear for all possible inputs, but many systems are approximately linear over a wide range of inputs.

The steady-state response of a linear (and time-invariant) system to a sine wave input is a sine wave of the same frequency. By dividing the output of the system by its input, we get a normalized result. When this is done over a range of frequencies, it is referred to as the frequency response. In a linear system, the frequency response is independent of the input amplitude.

The linearity of the tympanic membrane response in the intensity range of interest was investigated by measuring the tympanic membrane response at different intensities. Linearity would imply that for each dB increase in input sound pressure there will be a one dB increase in displacement. Measurements of varying intensities taken at the short process of the malleus will be used to investigate the linearity of the middle-ear response. The responses in this section were obtained from the same animal as in Section 5.5.1, and the reasons for selecting the short process are the same as discussed there. The results will be presented in Section 6.4.

5.6.4 Repeatability

When making measurements, it is important to keep in mind that the middle-ear response changes with time. By comparing consecutive measurements of vibrations at the umbo in live cats, Decraemer et al. (1990) showed that the total change in response within 6 minutes varied by between +5% and -10% in the frequency range of 130 to 25 000 Hz. Voss et al. (2000) found that the stability of stapes velocity measurements over time varied from ear to ear. Two measurements done an hour apart in one ear showed responses which were very similar, varying by a maximum of only 4 dB within a narrow frequency range. However, measurements on another ear showed low-frequency response changes of 6 dB after only 4 minutes (Figure 5.9). Voss et al. (2000) found that moistening the middle ear with saline solution often brought the response back to its original level (Figure 5.10). They also describe the existence of “unstable ears” for which large changes were recorded over short time intervals.

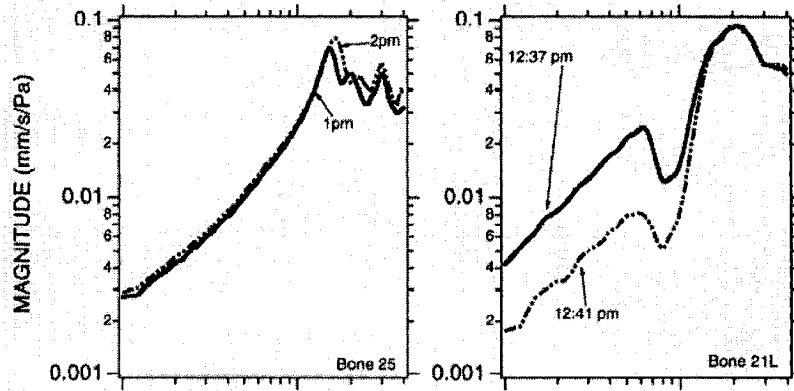


Figure 5.9 *Left:* Stable ear. Measurements taken one hour apart very similar. *Right:* Unstable ear. Measurements four minutes apart show large changes. (Modified from Voss et al., 2000)

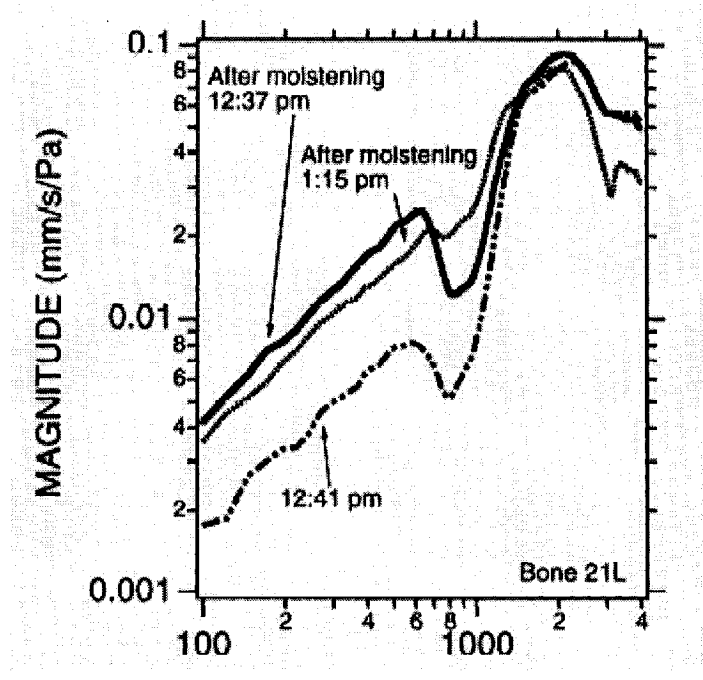


Figure 5.10 Remoistening the middle ear brought stapes responses back to normal levels. (Voss et al., 2000)

In order to test the repeatability of our frequency responses, we took repeat measurements every 10 – 20 minutes for up to 74 minutes in four rats. Measurements were first taken at the middle of the manubrium, followed by the umbo and then the short process, and this sequence was repeated throughout the time period. A sweeping sine signal from 250 – 10 000 Hz was used as the stimulus. Due to noise effects, responses between 250 and 1000 Hz will be ignored and the frequency responses in the range of 1 000 – 10 000 Hz will be presented (Section 6.5).

5.6.5 Variability

The results of studies on biological systems tend to be quite variable, and middle-ear frequency responses are no exception. Figure 5.11 shows umbo displacement curves from 15 human temporal bones as obtained by Goode et al. (1993). These results exhibit inter-ear variability of approximately 20 dB. Measurements of stapes velocities by Voss et al. (2000) on 18 temporal bones show similar amounts of variability (Figure 5.12).

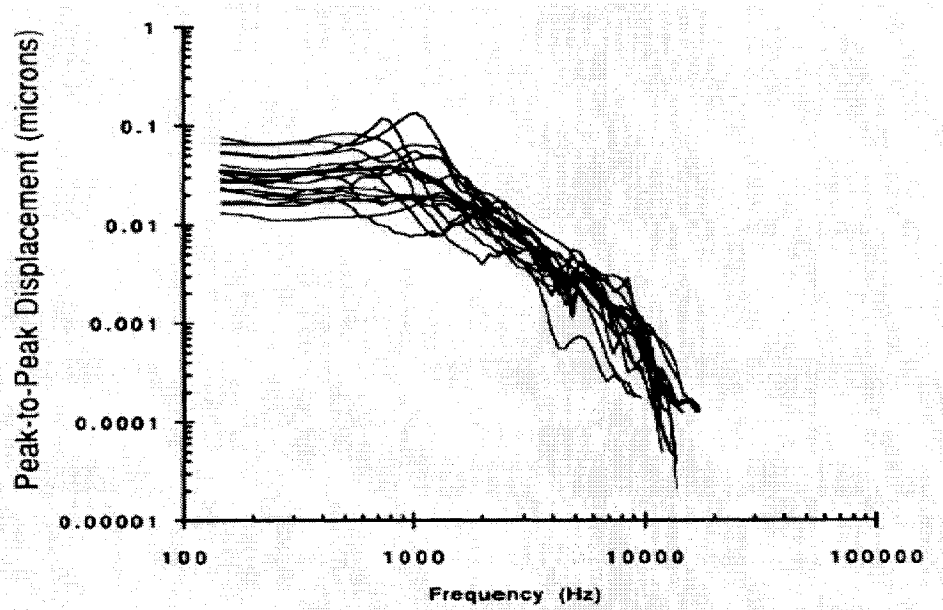


Figure 5.11 Umbo displacement curves for 15 human temporal bones. The thick line is the mean displacement curve. (Goode et al. 1993)

Measurements of 18 bones

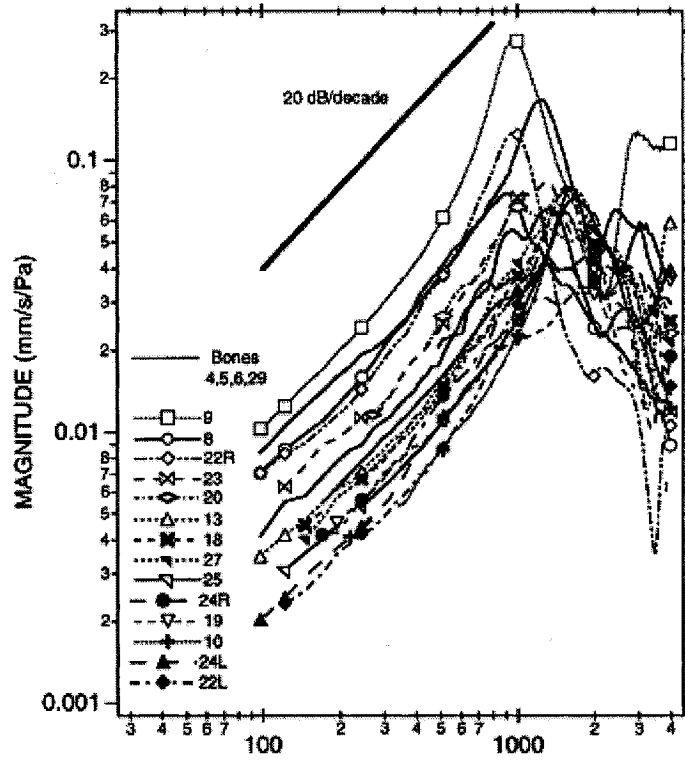


Figure 5. 12 Measurements of stapes velocity in 18 temporal bones (Voss et al., 2000).

The few previous studies of rat tympanic-membrane vibrations showed similar variability. Figure 5.13 shows umbo velocities as a function of sound frequency from five adult rats as measured by Doan et al. (1996). The inter-ear variability is in the 10-dB range at the lower to mid frequencies and increases with frequency. Our results will be plotted with those of Doan et al. (1996) in order to compare inter-animal variability at the umbo (Section 6.6).

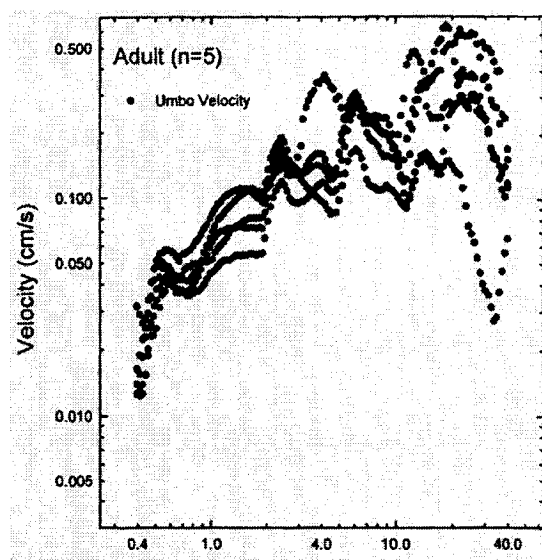


Figure 5.13 Umbo velocities from 5 adult rats. (Doan et al., 1996)

5.6.6 Characterizing TM Vibrations

Studies by Doan et al. (1996) and Bigelow et al. (1996, 1998) used technology similar to that used here to measure frequency responses of the rat tympanic membrane. They measured frequency responses only at the umbo. Although umbo measurements can reveal, in part, how the middle ear functions, they do not describe tympanic-membrane vibration patterns. To fully understand the vibrations of the TM and ossicles, one needs to measure displacements at points other than the umbo.

Frequency responses at seven points on the tympanic membrane were obtained in three rats (Figure 5.14). Three points were along the manubrium and the other four points were on the pars tensa. These measurements help to characterize the vibration patterns of the rat tympanic membrane. The frequency responses from the three points along the manubrium will be analyzed in an attempt to investigate the rigidity of the rat's manubrium (cf. Chapter 4.5). Frequency responses at the umbo and short process will also help in investigating the possible presence of two axes of rotation. According to Summers and Saunders (1982) (cf. Chapter 4.4), if there is a shift in rotational axis at high frequencies, the displacement of the umbo would increase relative to the displacements at the short process. Sections 6.7 and 6.8 present the results of these measurements.

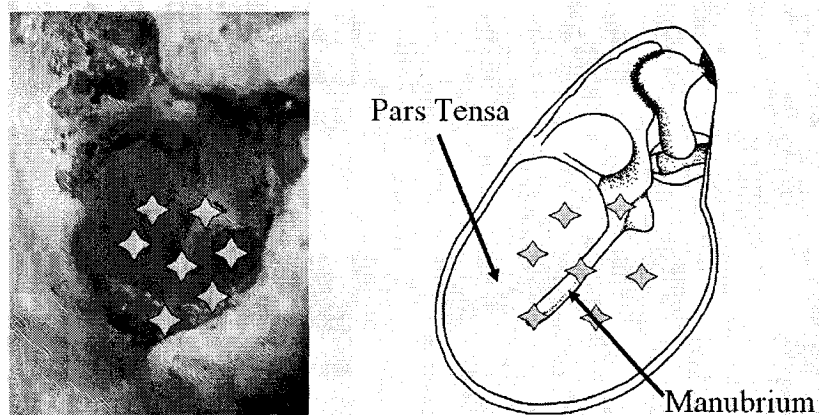


Figure 5.14 Frequency responses were measured at the seven points indicated by the stars. The image on the left is a photo of the middle ear; the drawing on the right is modified from Zimmer et al., 1994.

CHAPTER 6. Results

6.1 Introduction

In this chapter we will present the results of the investigations discussed in Chapter 5. We will start off by discussing the choice of excitation signal in Section 6.2. In Section 6.3, the noise floor is presented. The linearity of the middle ear is demonstrated in Section 6.4. The repeatability of our measurements and the variability of middle-ear frequency responses are discussed in Sections 6.5 and 6.6 respectively. The manubrium and tympanic-membrane vibrations will be characterized in Sections 6.7 and 6.8.

6.2 Excitation Signal

As discussed in Chapter 4, the previous vibration measurements in the rat (Doan et al., 1996; Bigelow et al., 1996; Bigelow et al., 1998) were all done with pure-tone sine waves as the stimulus. The time-consuming nature of this stimulation method does not allow for a high frequency resolution in reasonable amounts of time. The previous studies provided no more than 130 frequency points over a 40-kHz range. By applying a slowly sweeping sine wave, it is possible to obtain many thousands of readings, dramatically improving the frequency resolution.

Figure 6.1 shows that the pure-tone measurements coincide with the curves acquired with a sweeping stimulus. We see in this figure that the 45 pure-tone frequency responses are marked by an *X* and fall on the two curves representing the responses obtained with the sweeping stimulus before and after the pure-tone measurements. Recall from Section 5.5.1 that the pure-tone measurements took approximately 30 minutes. These results allow us to confidently use the sweeping stimulus, providing a higher frequency resolution in less time. Consequently, the results will give us more information and the effects of time-related changes in frequency response can be minimized.

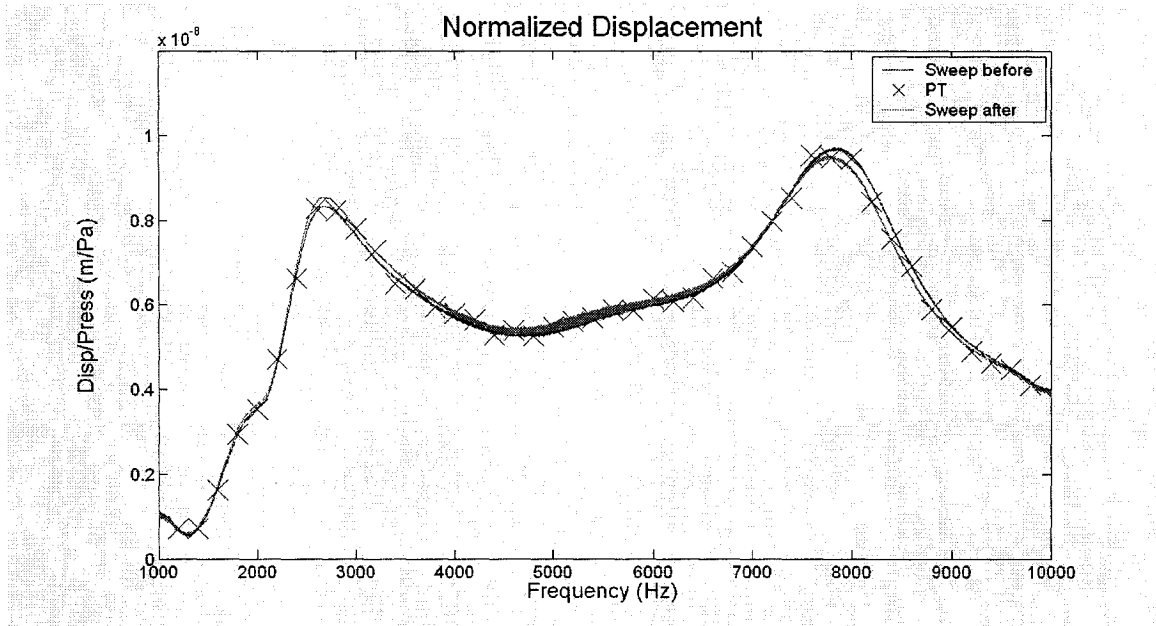


Figure 6.1 Pure-tone stimulus yields same results as sweeping-sine stimulus.

6.3 Noise Floor

Figure 6.4 shows frequency responses for the seven rats, measured at the short process, along with the noise-floor measurement. The signal-to-noise ratio for all rats is more than 20 dB above 1500 Hz except for Rat #2 for which the response experiences a sharp drop in amplitude at approximately 1 700 Hz. A combination of inherently small displacements at low frequencies and a larger noise-floor level at lower frequencies limits our ability to accurately measure displacements at frequencies below 1 kHz. For this reason, results below 1 000 Hz will be dropped.

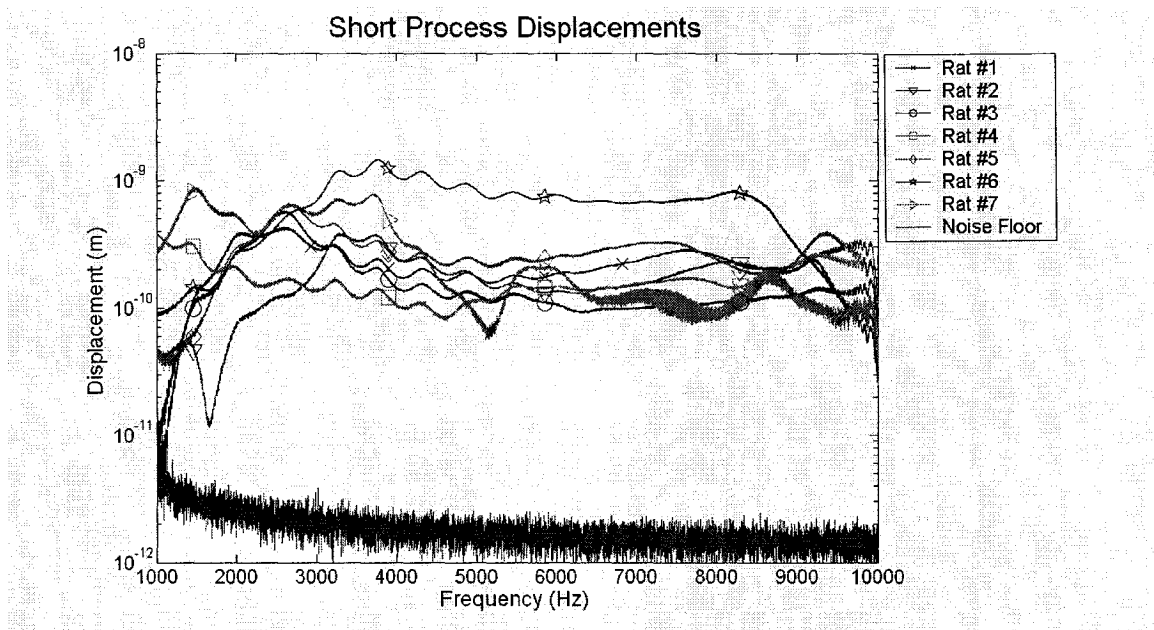


Figure 6. 2 Low-frequency noise and small displacements limit the ability to measure displacements below 1 kHz.

6.4 Linearity

Figure 6.3 shows the displacement of the short process as a function of varying sound pressure levels at 7 kHz. A straight line was fitted through the data points. The goodness of fit was evaluated using the R-square statistic. R-square takes values between 0 and 1, with a larger value indicating a better fit. The fitted line through the data points has a slope of 1.0 with an R-square value of 0.99, indicating linearity. Similar tests at 1 kHz, 2 kHz and 4 kHz were performed. Table 6.1 summarizes the findings. With all the data exhibiting slopes very close to one with good fits, we can say that the system behaves linearly. This finding allows us to interpret our measurements in terms of frequency responses computed as output/input ratios, and also allows us to confidently compare our results with frequency responses measured by other researchers at different sound pressure levels.

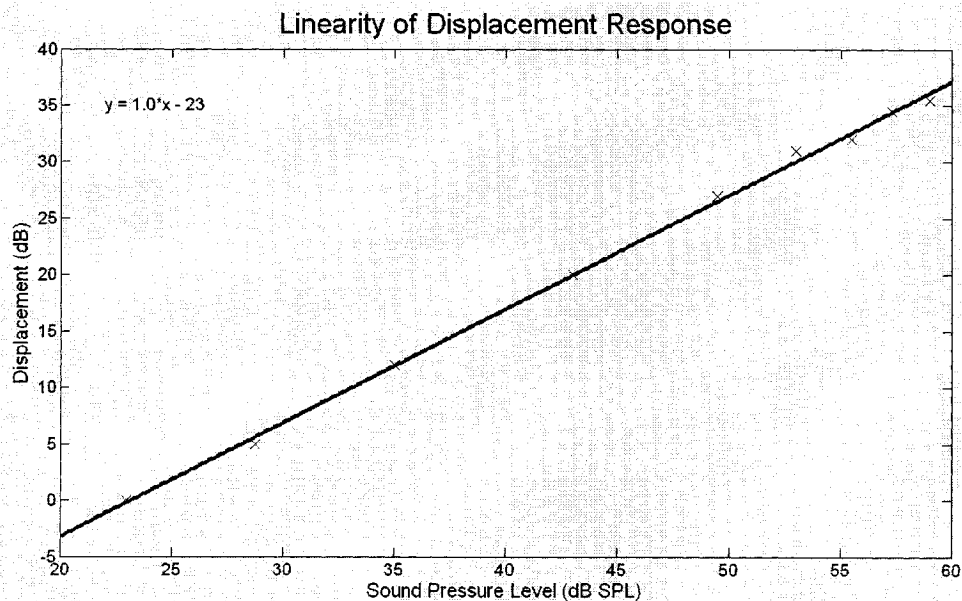


Figure 6.3 A line fitted through the data points describing displacements as a function of SPL.

Frequency	Slope	R-square
1000 Hz	1.01	0.99
2000 Hz	1.04	0.99
4000 Hz	0.98	0.99
7000 Hz	1.01	1.00

Table 6. 1 The slope and R-square values at four frequencies demonstrate the linearity of the system.

Figure 6.4 shows the sound pressure level as measured at the eardrum. The curve was obtained with a constant input voltage, but the sound pressure level varies between approximately 55 and 72 dB SPL over the frequency range of 1000 to 10 000 Hz. The stimulus used in obtaining this curve was the same one used for obtaining the frequency responses presented elsewhere in this chapter. The variation in sound pressure level is relatively smooth so we can be confident that the frequency responses will not behave erratically when normalized by dividing by the sound pressure level.

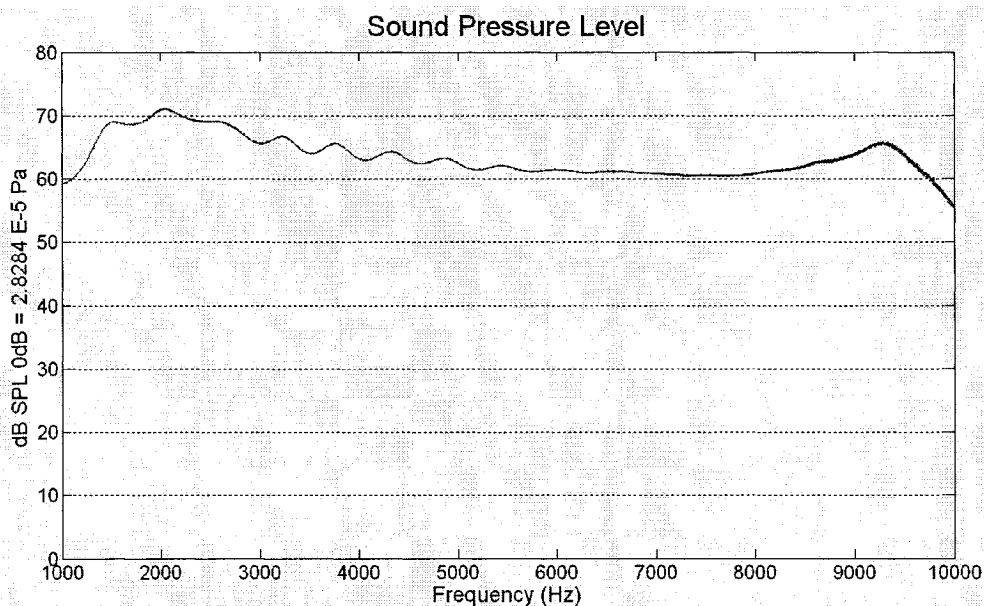


Figure 6. 4 Sound pressure level as measured at the tympanic membrane of Rat #5.

6.5 Repeatability

Repeat measurements from 4 rats are presented in order to determine the stability of the responses.

Frequency responses of the middle of the manubrium taken over a period of 74 minutes in Rat #4 are shown in Figure 6.5. The displacement curves don't show high variation over the 74 minute period, remaining within +4 and -6 dB of the original measurement throughout the frequency range. We can see that there is a big drop in amplitude after 10 minutes at low frequencies. The response drops even further after 30 minutes, but then increases and begins to stabilize. In contrast, at higher frequencies, the amplitude rises initially, before dropping and becoming relatively stable.

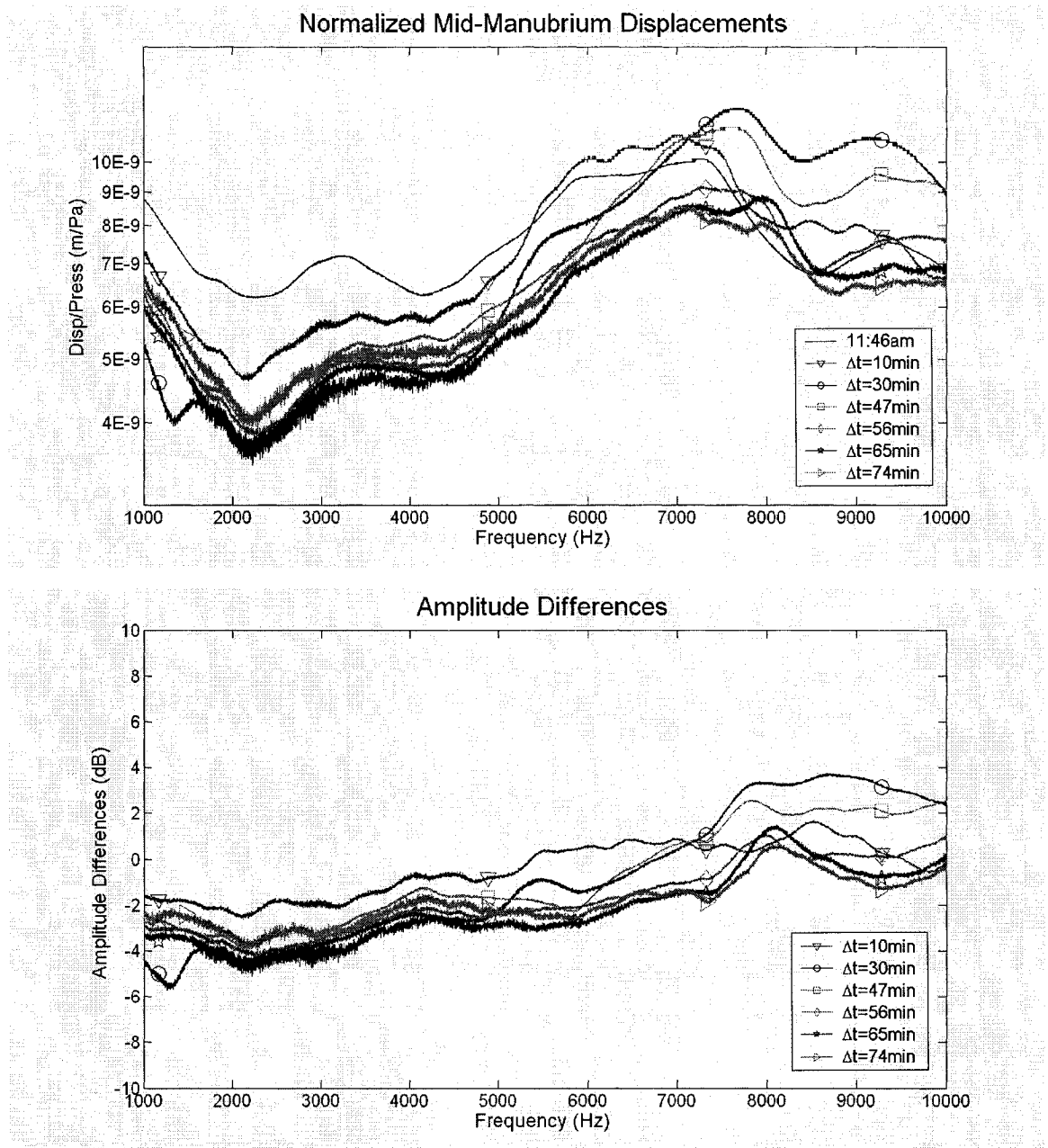


Figure 6. 5 *Top:* Repeat mid-manubrium displacement measurements for Rat #4. *Bottom:* Differences in amplitude (in dB) when compared to initial measurement.

The frequency responses taken at the middle of the manubrium for Rat #5 maintained a similar shape for approximately one hour (Figure 6.6). There was an overall shift downward in response and the higher-frequency peak drifted from ~7 300 Hz to ~8 000 Hz. The measurement taken after one minute is practically overlapping the original one, showing amplitude differences of less than 0.5 dB over most of the frequency range. The subsequent measurements remained within -4 and +6 dB, except below 1 500 Hz where the signals were very noisy. Responses measured at 12 and 40 minutes are similar to one another, as are the ones at 30 and 54 minutes.

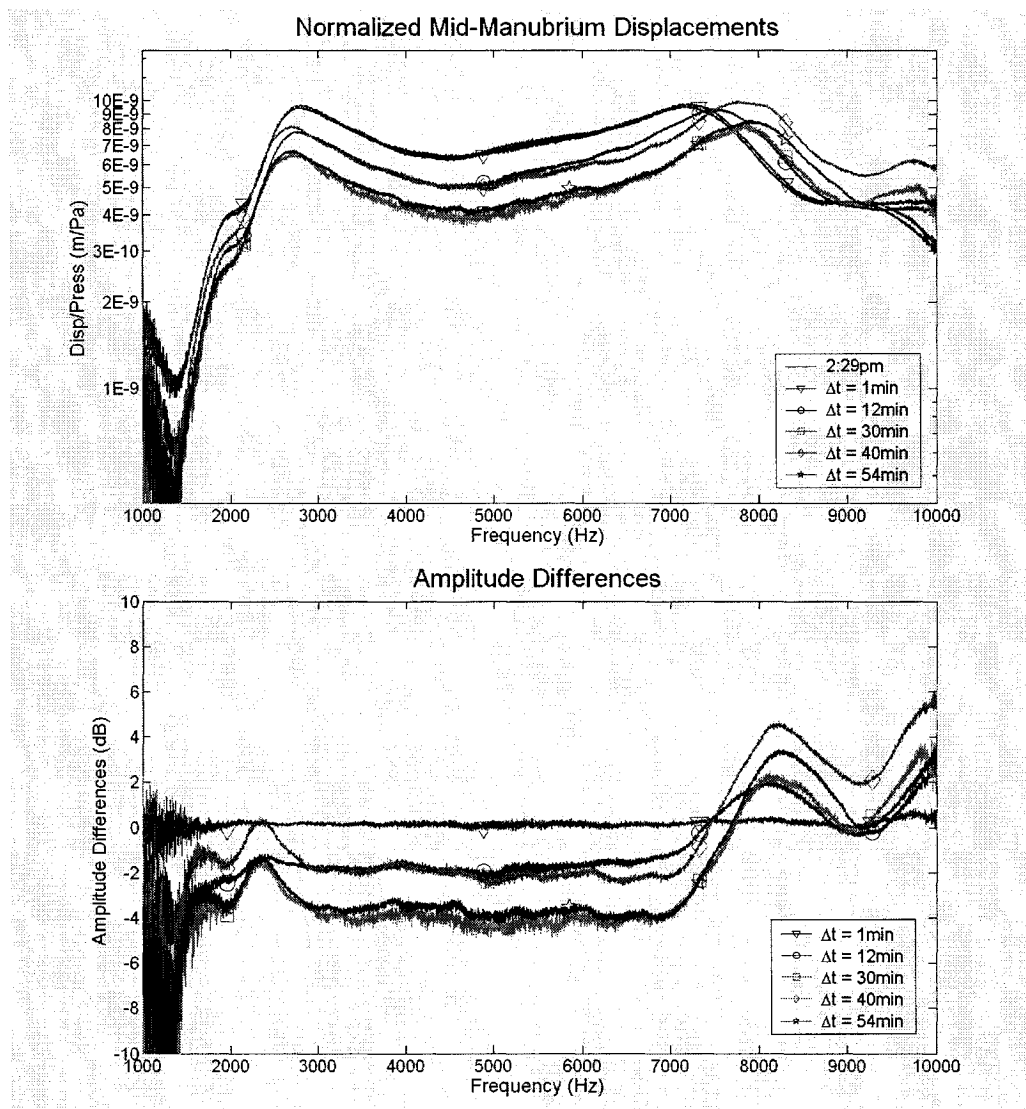


Figure 6. 6 *Top:* Repeat mid-manubrium displacement measurements for Rat #5. *Bottom:* Differences in amplitude (in dB) when compared to initial measurement.

Repeat measurements taken at the short process of Rat #6 are shown in Figure 6.7. The frequency response maintained a similar shape for approximately one hour although the displacements at the higher frequencies experienced changes in magnitude of up to 8 dB. A measurement taken one minute after the original one shows practically no deviations in amplitude over the frequency range. The system stabilizes at some point after the 21 minutes, with responses thereafter remaining within 1 dB of each other at all frequencies.

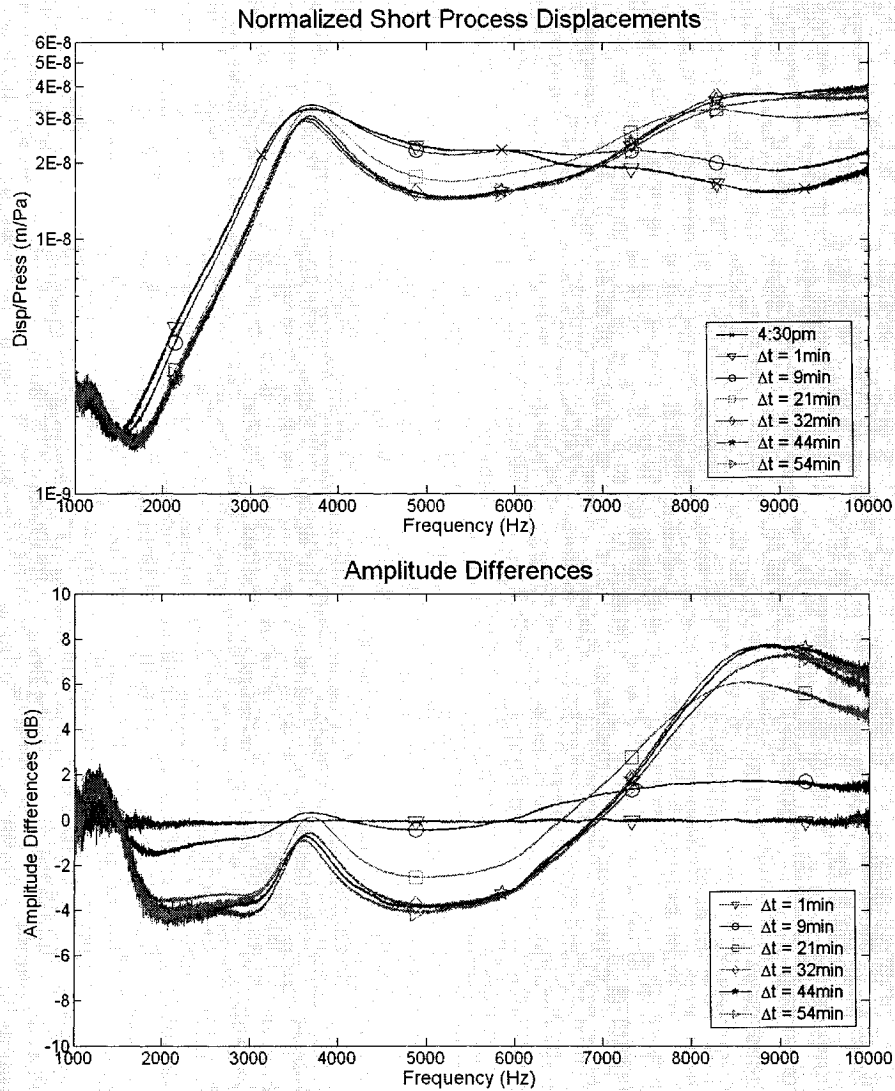


Figure 6. 7 *Top:* Repeat short process displacement measurements for Rat #6. *Bottom:* Differences in amplitude (in dB) when compared to initial measurement.

Repeated measurements at the umbo in Rat#7 are presented in Figure 6.8. The responses are similar below 5 kHz, but behave erratically above that. A measurement taken 2 minutes after the original one already shows changes in the range of 6 dB above 6 000 Hz. The system is very stable up to 18 minutes at frequencies up to 5.5 kHz.

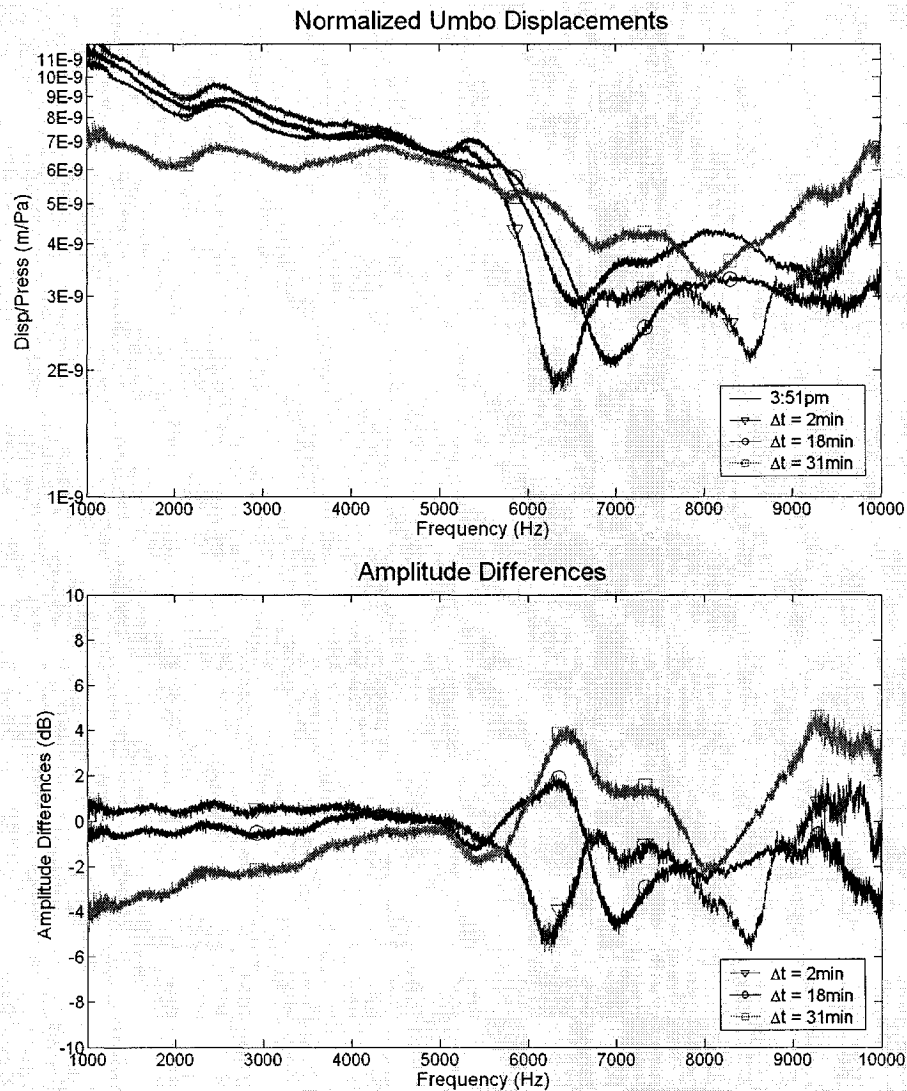


Figure 6.8 *Top:* Repeat umbo displacement measurements for Rat #7.
Bottom: Differences in amplitude (in dB) when compared to initial measurement.

As discussed in Chapter 5.6.4, the time-related changes in frequency response can probably be attributed in part to a drying out of the tympanic membrane, ligaments of the ossicular chain and middle-ear muscles in all animals.

6.6 Inter-Animal Variability at the Umbo

Inter-animal variability causes problems when it comes to making generalized conclusions about the function of the middle-ear. Figure 6.9 shows the normalized umbo displacements for the seven rats studied here. Responses shown for Rats #4 – #7 are the first measurements taken for each rat. Variability is in the 40 dB range from 1 000 – 2 000 Hz and in the 20 dB range from 2 000 – 10 000 Hz. The least amount of variability is at ~2 500 Hz. If the response from Rat #6, which is much higher than all the others above 3 kHz, is excluded, the variability is decreased to within 10 dB from 3 to ~6 kHz, and 15 dB above that. The inter-ear variability above 2 kHz falls within the 20 dB range experienced by Goode et al. (1993) and Voss et al. (2000) in their studies on human temporal bones. We can see from Figure 6.9 that Rat #1 behaves similarly to Rat #3; as do Rats #4 & #7; and Rats #2, #5 and (to a lesser extent) #6 also behave similarly.

Figure 6.10 shows the results from our seven rats plotted with those of the five rats from Bigelow et al.'s (1996) study. The figure was created by scanning the results from their paper and superimposing our frequency responses. The curves presented in this figure represent velocity frequency responses, as opposed to the displacement frequency responses in Figures 6.5 – 6.9 and 6.11 – 6.20. Velocities at frequencies lower than ~3 kHz are much lower in our study for five of the rats. The amplitudes are, however, in the same range as those of Bigelow et al. (1996) results between 3 and 10 kHz. The other two rats (Rats #4 and #7) have responses similar to those of Bigelow et al. throughout the frequency range. The response from Rat #6, which is much higher than our other rats above 3 kHz, is very similar to one of the rat responses presented by Bigelow et al. from 3 to 4 kHz.

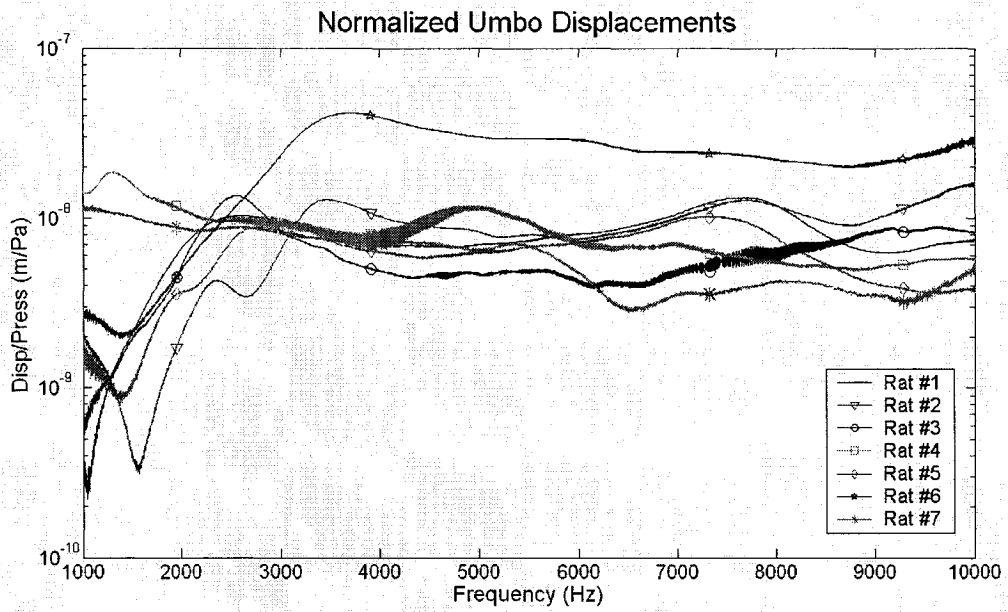


Figure 6. 9 Normalized displacements for all seven rats are plotted together. Inter-ear variability ranges from 20 dB to 40 dB.

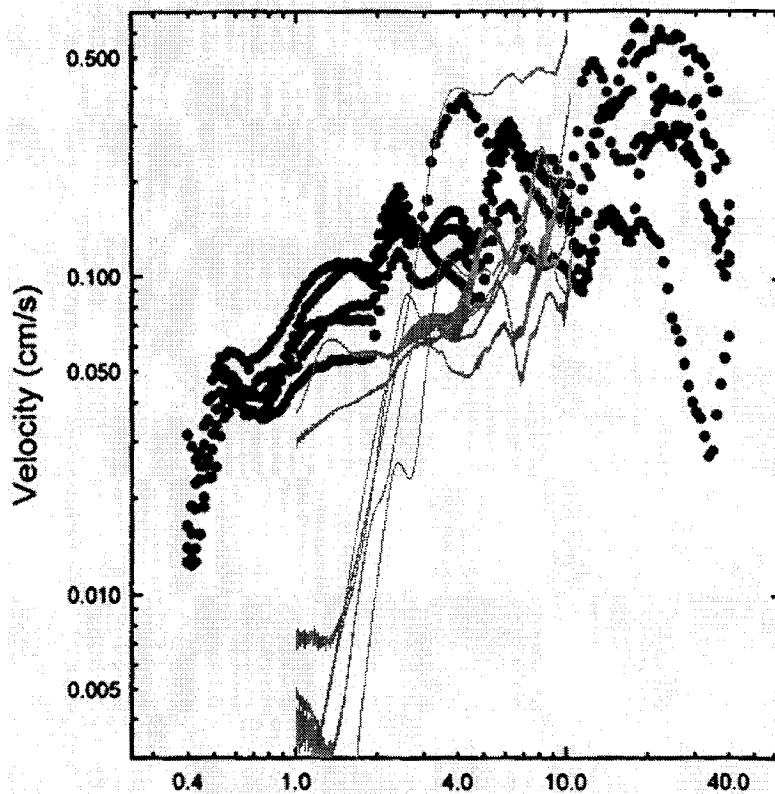


Figure 6. 10 The variability of our results (grey) is compared with the variability of 5 rats from a previous study (black). (Modified from Bigelow et al., 1996)

According to the interpretation of the authors of the previous studies, the measurements at the umbo indicate that the middle-ear frequency responses show two characteristic peaks in the range of frequencies we are studying. Table 6.1 summarizes the findings of the previous studies and includes the characteristic peaks found in our rats. Rats #6 and #7 each had what we considered a weak peak in the range of interest which is indicated by an asterisk in the table. Although no two rats are exactly the same, Rats #1, #2 and #5 seem to fit the pattern described by the previous studies.

	Low-frequency peak	High-frequency peak
Doan et al., 1996	2300	6300
Bigelow et al., 1996	2500	5500
Bigelow et al., 1998	1500	5000
Rat #1	2500	7500
Rat #2	3500	7800
Rat #3	2500	9500
Rat #4	1300	5000
Rat #5	2800	7300
Rat #6	3800	6000*
Rat #7	2500*	8200*

Table 6. 2 Umbo frequency response peaks from previous studies and present work. Asterisk indicates a weak peak.

6.7 Characterizing Manubrial Vibrations

Figures 6.11 – 6.17 show the frequency responses for multiple points on the manubrium. The measurements for Rats #1 – #3 were done at the umbo first, then at the middle of the manubrium and finally at the short process. For Rats #4 – #7, the first measurement was at the middle of the manubrium, followed by the umbo and the short process. In Rats #1, #2, #4 and #6, the umbo displaces more than the middle of the manubrium, which in turn displaces more than the short process. These four rats (Rats #1, #2, #4 and Rat #6) are examples consistent with an assumption of a rigid

manubrium rotating around an anterior-posterior axis. Whereas the general shapes of the curves are the same for Rats #1, #2 and #6, this is not the case for Rat #4.

Rats #3, #5 and #7 have behaviours different than the other four rats. For Rat #3, the middle of the manubrium seems to have displacement magnitudes similar to those of the umbo up to 2 700 Hz. Above this frequency, the mid-manubrial displacements are slightly larger than those of the umbo. The short process has the smallest displacements and the shapes of all three curves are similar. In Rat #5, the middle of the manubrium displaces more than the umbo up until about 6 800 Hz. The responses are stable in two regions, one below ~5 kHz and the other between 7 500 and 8 500 Hz, and experience transitions elsewhere. Above approximately 8 500 Hz, the short process displacements increase rapidly, while those at the umbo and mid-manubrium continue to decrease. For Rat #7, we can see that the umbo and middle of the manubrium have similar displacements below 5 kHz. The short process has a sharp peak at 3 500 Hz causing it to displace more than the umbo and mid-manubrium between ~2 300 and ~4 300 Hz. Above 6 kHz, the middle of the manubrium displaces more than the umbo. The short process response does not resemble the umbo and mid-manubrium displacements, and goes through several transitions. Although there is a suspicion of manubrial bending in these rats, given that the middle of the manubrium displaces more than the umbo at certain frequencies, this could also be explained by another axis of rotation that we have not accounted for. It is also important to consider that, as suggested by Decraemer et al. (1991, 1994) and Decraemer and Khanna (1994), there may not even be a fixed axis of rotation.

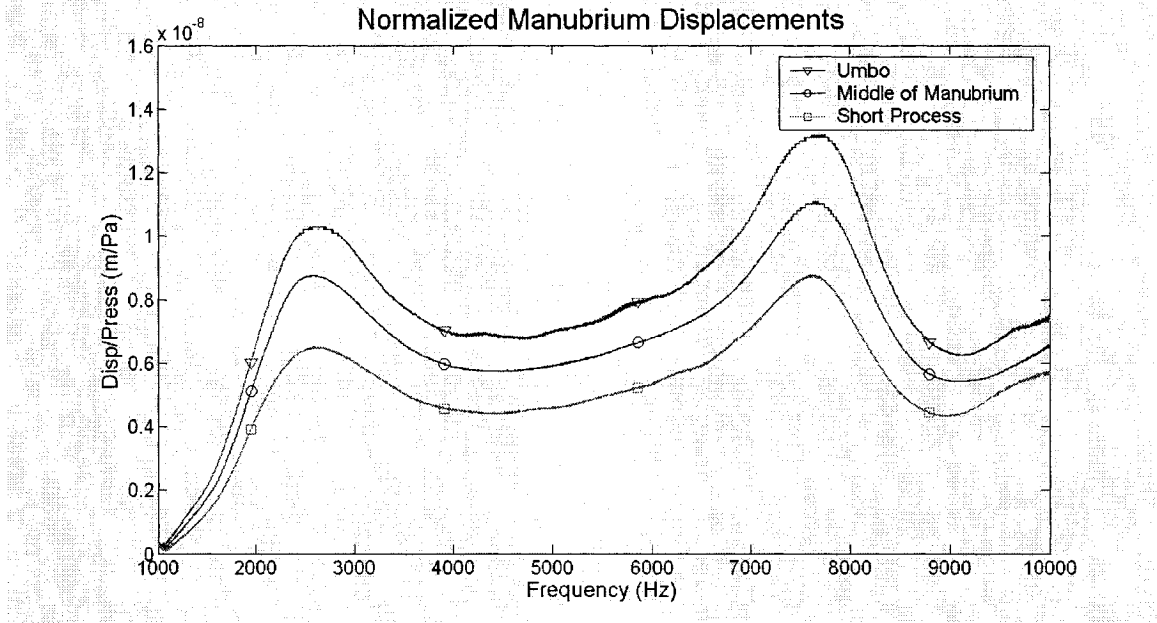


Figure 6.11 Manubrial Displacements for Rat #1

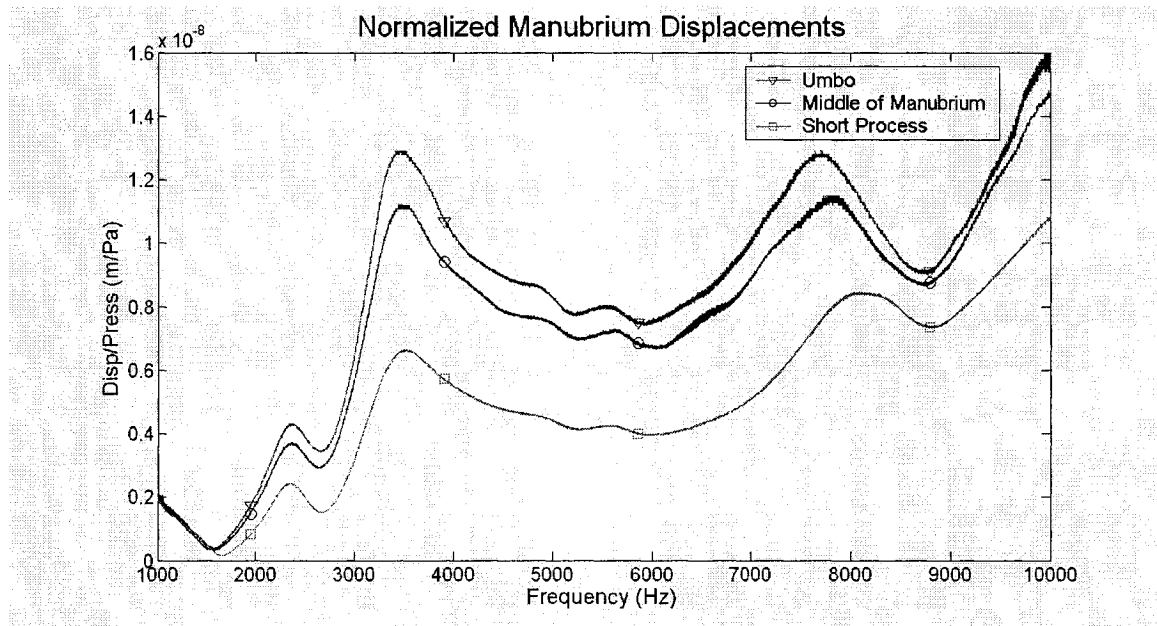


Figure 6.12 Manubrial displacements for Rat #2

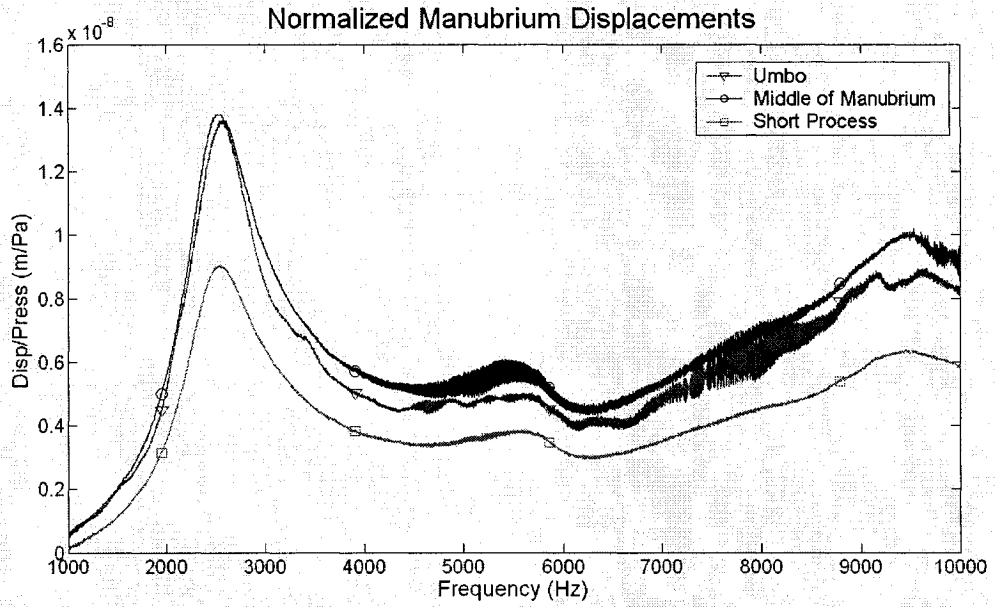


Figure 6. 13 Manubrial displacements for Rat #3

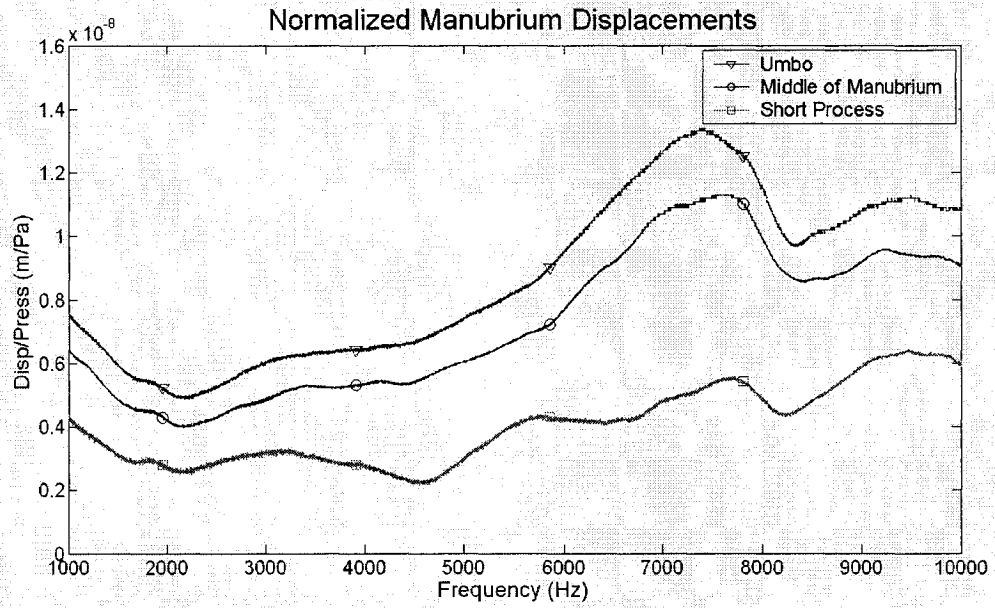


Figure 6. 14 Manubrial displacements for Rat #4.

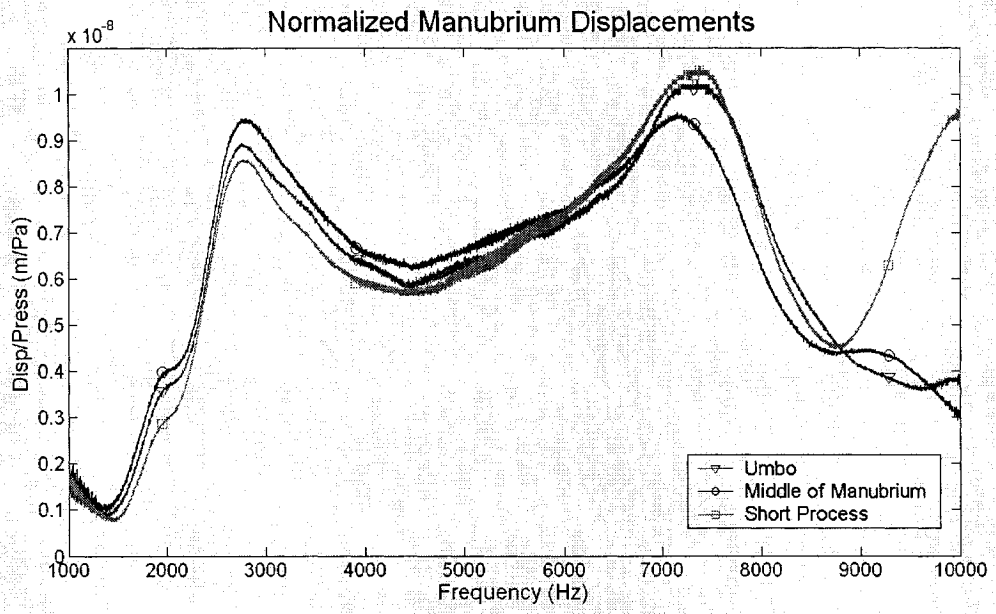


Figure 6. 15 Manubrial displacements for Rat #5.

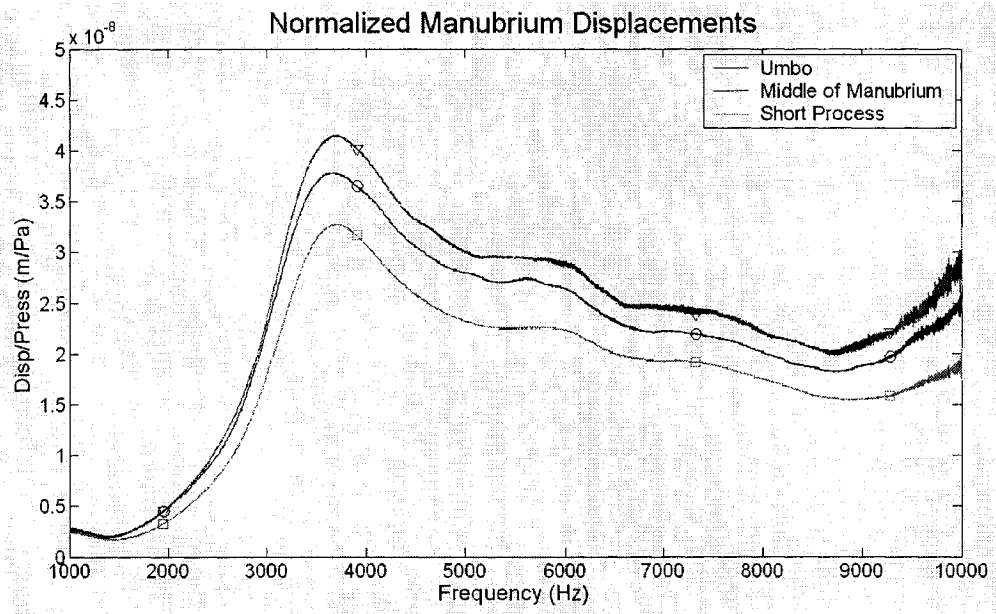


Figure 6. 16 Manubrial displacements for Rat #6.

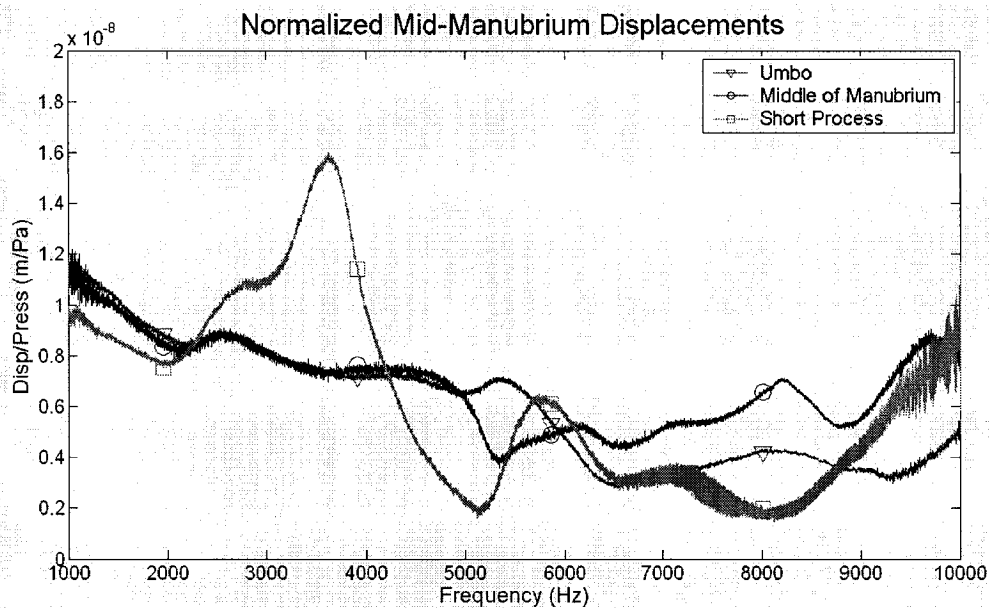


Figure 6.17 Manubrial displacements for Rat #7.

According to Saunders and Summers (1982) (cf. Chapter 4.4) a changing of modes from the low-frequency to the high-frequency mode in the microtype ear would be characterized by the short process displacements becoming small when the high-frequency axis passes near it. They predict, however, that the changing of modes in mice occurs at 18 kHz. Given the limited frequency range presented here, we expect our results to compare to the low-frequency mode described by Saunders and Summers (1982). In this mode, we expect short-process and umbo displacements to be similar. The results of Saunders and Summers show a short-process-to-umbo velocity ratio of ~ 0.8 . In our results, the responses from Rats #3, #5 and #6 show that umbo and short process displacements are quite similar with ratios of 0.75, 1, and 0.8 respectively. Rat #1 has a ratio of approximately 0.65 and Rat #2 shows short process displacements half as large as umbo displacements (ratio of 0.5). In Rat #4 the ratio fluctuates between 0.3 and 0.6. In Rat #7 the umbo and short process do not have similar displacement responses with the ratio fluctuating between 0.3 and 2.2. The fact that most animals have short-process-to-umbo displacement ratios that are significantly less than one implies that the low-frequency axis is not parallel to the manubrium, as Saunders and Summers (1982) suggested.

6.8 Characterizing TM Vibrations

Pars-tensa frequency responses were measured in Rats #1 to #3 and are presented in Figures 6.18 – 6.20. For Rat #1, we can see that points on the posterior side of the tympanic membrane tend to displace more than anterior ones. Also, the anterior displacements are similar in magnitude to those of the umbo, whereas the posterior ones are up to six times larger. Frequency responses from Rat #2 show that posterior displacements are larger than anterior ones up to ~8 300 Hz, at which point the infero-posterior displacements drop. All four points displace more than the umbo throughout the frequency range. The results for Rat #3 show that the infero-posterior and infero-anterior displacements are similar in magnitude, with the superio-posterior displacements being the largest and the supero-inferior being the smallest. Umbo displacement magnitudes are comparable to the supero-inferior displacements. We can see from all three rats that displacements on the same side of the manubrium are more similar to each other than they are to points on the other side of manubrium. For example, two anterior responses are more similar to each other than an anterior response is to a posterior response.

For Rat #1, the infero-anterior measurement begins to behave differently from the other three points above about 6kHz. In the responses for Rat #2, the infero-posterior measurement begins to behave differently at about 7 kHz. For Rat #3, the four responses are similar up to approximately 6 kHz. The similarly shaped frequency responses at the four points on each pars tensa show that the vibration patterns are rather simple at these frequencies.

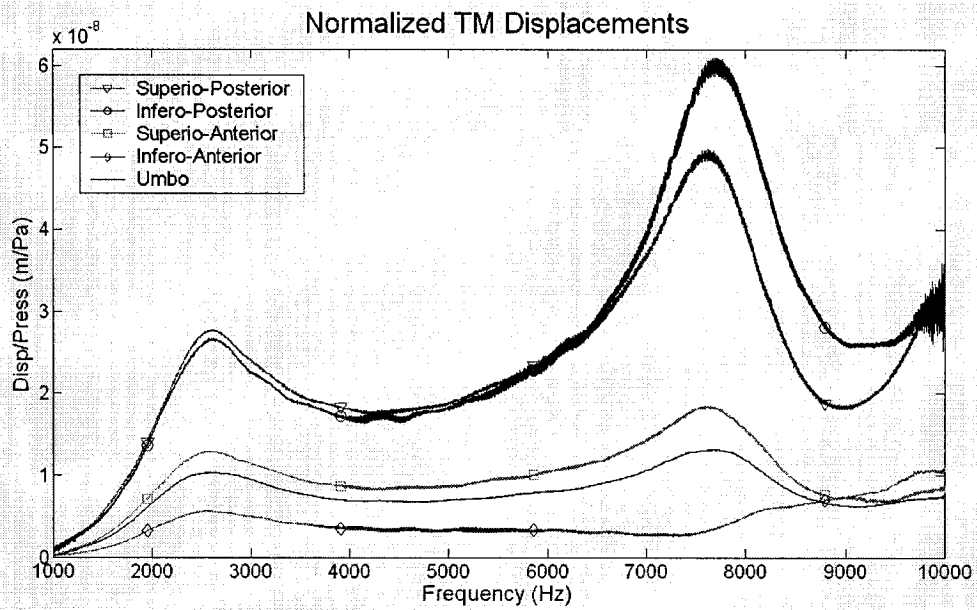


Figure 6. 18 Tympanic membrane displacements for Rat #1

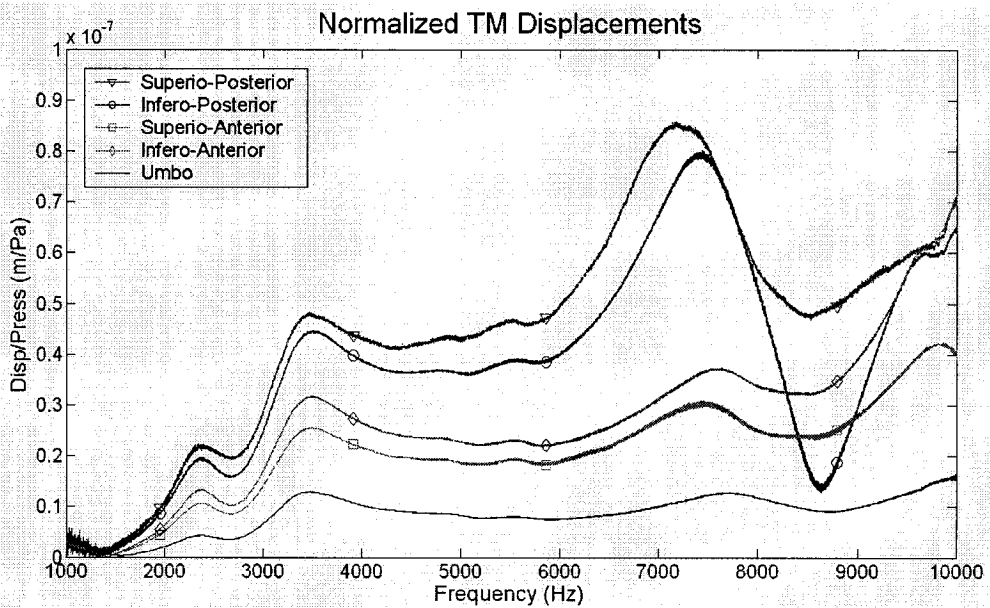


Figure 6. 19 Tympanic membrane displacements for Rat #2

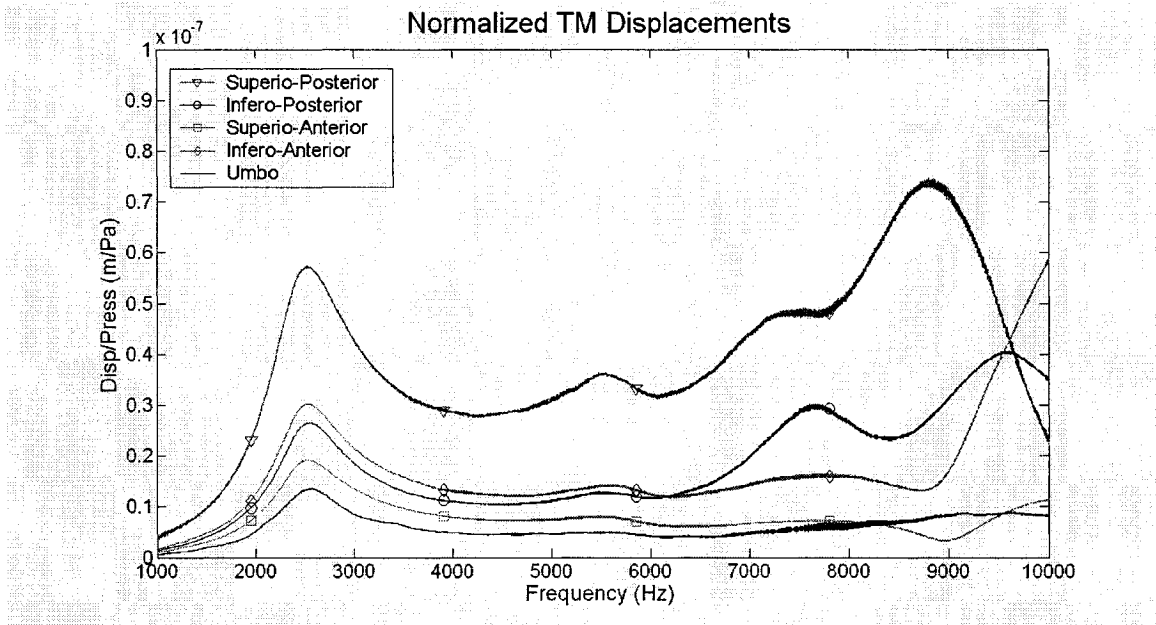


Figure 6. 20 Tympanic membrane displacements for Rat #3

CHAPTER 7. Conclusions

7.1 Summary

This study is the first to present measurements of rat tympanic-membrane and manubrium vibrations at points other than the umbo. Furthermore, the use of the sweeping-sinusoid stimulus allowed us to obtain a higher frequency resolution than in previous studies. We can also expect more reliable results because of the reduction of time-related changes.

We have provided a measure of the noise floor and confirmed the linearity of the rat tympanic membrane for sound pressure levels between 23 and 59 dB SPL. The repeatability of the rat's middle-ear response over time was also investigated. Inter-animal variability at the umbo was presented and compared to other studies. The vibration modes of the tympanic membrane and manubrium were also investigated.

Fleischer (1978) characterised the middle ears of the rat and mouse as being 'microtype': the manubrium is fused to the tympanic ring at the gonial bone, and there is a large mass at the head of the malleus called the *orbicular apophysis*. Fleischer analysed an enlarged mechanical model and hypothesised that there are two axes of rotation in microtype ears: a low-frequency axis approximately parallel to the manubrium, and a high-frequency axis approximately perpendicular to the manubrium. Saunders & Summers (1982) measured vibrations at the short process and umbo in the mouse. They found, consistent with Fleischer's hypothesis, that at low frequencies the short-process and umbo displacements were similar, with a ratio of ~ 0.8 . By ~ 10 kHz the ratio was becoming smaller and by ~ 18 kHz it had dropped below 0.5, consistent with a transition to Fleischer's high-frequency axis. Since the rat ear is larger than that of the mouse, one might expect the transition between modes to occur at a lower frequency.

Our measurements show short-process/umbo ratios of 0.75 and higher in three rats, consistent with the low-frequency findings of Saunders & Summers in the mouse, and with Fleischer's hypothesis of a low-frequency axis parallel to the manubrium. Our observed ratio was significantly lower in three other rats, however, suggesting that the axis was not parallel to the manubrium in those ears.

The frequency responses that we observed at four points on the eardrum are similar in shape to those observed on the manubrium. This suggests that the vibration pattern of the rat eardrum is still simple up to 10 kHz and has not yet broken up into multiple out-of-phase regions.

By characterizing the manubrial and pars tensa vibrations, we have provided important information that will help in better understanding the function of the middle ear.

7.2 Future Work

7.2.1 Introduction

This study is the first in our lab that has made use of laser Doppler vibrometry to characterize middle-ear vibrations. The use of rats is also new for our lab. As such, a number of refinements are needed.

7.2.2 Experimental Methodology

The issue of repeatability needs to be investigated further in order to determine if animals are actually different and to see if age, weight and sex may have an effect. Constant moisturizing during the experiments and the placement of a moist cotton ball in the sound chamber can be investigated as methods of keeping the middle ear from drying out. In order to determine whether or not the specimen as a whole was vibrating, measurements need to be taken at a point where we would not expect a response, such as the external ear-canal wall.

The laser vibrometer is calibrated by the manufacturer with a specified flat sensitivity and 0° phase in the audio band. Although the probe-tube microphone system is also calibrated at the factory, it is only calibrated for sound pressure and not for phase. It is therefore necessary to calibrate the microphone for phase in order to obtain a more complete characterization of the tympanic-membrane vibrations.

Given the limitations of the sound-delivery and probe-microphone systems used, the range of frequencies studied was restricted to 10 kHz. Increasing this range would allow us to investigate the vibration patterns at higher frequencies and the correctness of the hypothesized micro-type axes of rotation.

7.2.3 Understanding of Middle-Ear Mechanics

Our experience has confirmed that the middle-ear structures of the rat are, in fact, easily approachable. Since the rat is also considerably less expensive than most other mammalian experimental animals, we believe that it could be of great value in ear research. It will be necessary, however, to investigate the feasibility of experiments involving modification of the middle-ear structures, in the case of prosthetic evaluation for example, given the smaller size of the rat ear. Measurements at other important points, such as the stapes, should also be made. It would also be interesting to pursue the questions regarding the modes of vibration of the manubrium and tympanic membrane, as well as the possible bending of the manubrium, by measuring more points and measuring at different angles.

Finite-element analysis provides a way of producing good mathematical models of the middle ear. The results provided in this work can be used to validate such a model and, consequently, provide more insight into how the tympanic membrane and middle ear behave mechanically.

Measuring the geometry of the middle ear for each specimen is important. This can be done by obtaining microscopic computed-tomography scans of the ear (e.g.,

Decraemer et al., 2003). This would allow us to determine the relative positions of the measurement points accurately. Micro-computed tomography scans will also allow us to try to identify reasons for variability by investigating anatomical differences. It can also be useful when it comes to creating a finite-element model.

Single-direction measurements are not sufficient if one wants to determine whether there is a fixed axis of rotation, and how the axis is positioned and oriented. Therefore, in order to properly characterize the motion of the malleus, one would have to measure the three-dimensional motion of the malleus at a number of points. Decraemer et al. (1994) accomplished this by changing the observation angle with a two-axis goniometer system.

Whereas the previous works (Saunders and Summers, 1982; Bigelow et al., 1996, 1998; Doan et al., 1996) were done on *in vivo* specimens, our measurements were done *post mortem*. Although these measurements are thought to offer a good representation of the function of the middle ear, it is important that at least some future work be done on live subjects.

References

- Agilent (2002): "Fundamentals of Signal Analysis Series: Introduction to Time, Frequency and Modal Domains - Application Note 1405-1"
http://www.educatorscorner.com/media/AN_1405_1.pdf
- Agilent (2002): "Fundamentals of Signal Analysis Series: Understanding Dynamic Signal Analysis - Application Note 1405-2"
http://www.educatorscorner.com/media/AN_1405_2.pdf
- Beccari E., Molinengo L. (1958): "Osservazioni sulla sensibilita' uditiva del ratto alle diverse frequenze di stimolazione e sulla capacita' discriminativa della intensita'," *Soc. Ital. Biol. Sperim. Boll.* 34: 368-371
- Békésy G.v. (1960): *Experiments in hearing*. E.G. Wever (Ed.), (McGraw Hill, New York)
- Berge H.v.d., Geest A.v., Rensema J.W. (1990): "Three-dimensional graphic reconstruction of the tympanic bulla of the rat with special reference to the middle ear muscles," *Acta Otolaryngol* 110(3-4): 253-261
- Bigelow D.C., David K., Saunders J.C. (1998): "Effect of healed tympanic-membrane perforations on umbo velocity in the rat," *Ann Otol Rhinol Laryngol* 107: 928-934
- Bigelow D.C., Swanson P.B., Saunders J.C. (1996): "The effect of tympanic membrane perforation size on umbo velocity in the rat," *Laryngoscope* 106(1): 71-76
- Buunen T.J.F., Vlaming M.S.M.G. (1981): "Laser-Doppler velocity meter applied to tympanic membrane vibrations in cat," *J Acoust Soc Am* 58: 223-228
- Crowley D., Hepp-Reymond M., Tabowitz D., Palin J. (1965): "Cochlear potentials in the albino rat," *J Auditory Res* 5: 307-316
- Cummings C.W., Haughey B.H., Thomas J.R., Harker L.A., Robbins K.T., Schuller D.E., Flint P.W., Richardson M.A. (2005): *Cummings Otolaryngology: Head and Neck Surgery*, 4th ed. (Mosby Inc., St. Louis)
- Decraemer W.F., Dirckx J.J.J., Funnell W.R.J. (2003): "Three-dimensional modelling of the middle-ear ossicular chain using a commercial high-resolution x-ray CT scanner," *JARO* 4(2): 250-263
- Decraemer W.F., Khanna S.M. (1994): "Modelling the malleus vibration as a rigid body motion with one rotational and one translational degree of freedom," *Hearing Research* 72: 1-18

- Decraemer W.F., Khanna S.M., Funnell W.R.J. (1989): "Interferometric measurement of the amplitude and phase of tympanic membrane vibrations in cat," *Hearing Research* 38: 1-18
- Decraemer W.F., Khanna S.M., Funnell W.R.J. (1990): "Heterodyne interferometer measurements of the frequency response of the manubrium tip in cat," *Hearing Research* 47: 205-218
- Decraemer W.F., Khanna S.M., Funnell W.R.J. (1991): "Malleus vibration mode changes with frequency," *Hearing Research* 54: 305-318
- Decraemer W.F., Khanna S.M., Funnell W.R.J. (1994): "A method for determining three-dimensional vibration in the ear," *Hearing Research* 77: 19-37
- Doan D.E., Igic P.G., Saunders J. (1996): "Middle-ear development VII: Umbo velocity in the neonatal rat," *J Acoust Soc Am* 99 (3), 1566-1572
- Donaldson J.A., Duckert L.G., Lampert P.M., Rubel E.W. (1992): *Surgical Anatomy of the Temporal Bone*, 4th ed. (Raven Press, New York)
- Drain L.E. (1980): *The Laser Doppler Technique*, (John Wiley and Sons Ltd., Norwich)
- Feldman A.S., Wilber L.A. (1976): *Acoustic Impedance and Admittance – The Measurement of Middle Ear Function*, (The Williams and Wilkins Company, Baltimore)
- Fleischer G. (1978): "Evolutionary Principles of the Mammalian middle ear," *Adv Anat Embryol Cell Biol* 55: 1-70
- Funnell W.R.J. (1996): "Low-frequency coupling between eardrum and manubrium in a finite-element model," *J Acoust Soc Am* 99(5): 3036-3043
- Funnell W.R.J., Khanna S.M., Decraemer W.F. (1992): "On the degree of rigidity of the manubrium in a finite-element model of the cat eardrum," *J Acoust Soc Am* 91(4 Pt 1): 2082-2090
- Gilad P., Strikman S., Hillman P. (1967): "Application of the Mössbauer method to ear vibrations," *J Acoust Soc Am* 41: 1232-1236
- Goode R.L., Ball G., Nishihara S. (1993): "Measurement of umbo vibration in human subjects – method and possible clinical applications," *Am J Otol* 14(3): 247-251
- Goode R.L., Ball G., Nishihara S. (1996): "Laser Doppler vibrometer (LDV) – A new clinical tool for the otologist," *Am J Otolaryngol* 17: 813-822
- Guinan J.J., Peake W.T. (1967): "Middle-ear characteristics of anesthetized cats," *J Acoust Soc Am* 41: 1237-1261

- Gummer A.W., Smolders J.W.T., Klinke R. (1989): "Mechanics of a single-ossicle ear: I. The extra-stapedius of the pigeon," *Hearing Research* 39: 1-14
- Hariharan P. (1992): *Basics of Interferometry*, (Academic Press, Sydney)
- Hariharan P. (2003): *Optical Interferometry*, 2nd ed. (Academic Press, Sydney)
- Helmholtz, H.F.L. (1869): "Die Mechanik der Gehörknöchelchen und des Trommelfells," *Pflügers Archiv Physiol* 1, 1-60
- Helmholtz, H.F.L. (1877): *Die Lehre von den Tonempfindungen*, 4th ed. (Verlag von Fr. Vieweg u. Sohn, Braunschweig)
- Huber A.M., Schwab C., Linder T., Stoeckli S.J., Ferrazzini M., Dillier N., Fisch U. (2001): "Evaluation of eardrum laser Doppler interferometry as a diagnostic tool," *Laryngoscope* 111: 501-507
- Ishii H., Kimura K., Harada O. (1964): "Stress and auditory characteristics of the rat," *Ann Otol Rhinol Laryngol* 73: 948-956
- Judkins R.F., Li H. (1997): "Surgical anatomy of the rat middle ear," *Otolaryngol Head Neck Surg* 117: 438-447
- Khanna S.M. (1970): "A holographic study of tympanic membrane vibrations in cats," Ph.D. thesis, Columbia University
- Khanna S.M., Tonndorf J. (1972): "Tympanic membrane vibrations in cats studied by time-averaged holography," *J Acoust Soc Am* 51: 1904-1920
- Mayinger F., Feldmann O. (2001): *Optical measurements: Techniques and applications*, 2nd ed. (Springer, New York)
- Rat Genome Sequencing Consortium (2004): "Genome sequence of the Brown Norway rat yields insights into mammalian evolution," *Nature* 428: 493-521
- Relkin E.M., Saunders J.C. (1980): "Displacement of the malleus in neonatal golden hamsters," *Acta Otolaryngol* 90: 6-15
- Rosowski J.J. (1990): "Cadaver Middle Ears as Models for Living Ears: Comparisons of Middle Ear Input Immittance," *Ann Otol Rhinol Laryngol* 403-412
- Rosowski J.J., Brinsko K.M., Tempel B.I., Kujawa S.G. (2003): "The aging of the Middle Ear in 129S6/SvEvTac and CBA/CAJ Mice: Measurements of Umbo Velocity, Hearing Function, and the Incidence of Pathology," *JARO* 04: 371-383

- Rosowski J.J., Huber A.M., Ravicz M.E., Goode R.L. (2004): "Are temporal bones useful models of human middle-ear mechanics?" 27th ARO Midwinter Meeting, Daytona Beach, FL, USA
- Ruggero M.A., Temchin A.N. (2003): "Middle-ear transmission in humans: wide-band, not frequency-tuned?" *Acoustic Research Letters Online* 4(2): 53-58
- Ruggero M.A., Rich N.C., Robles L., Shivapuja B.G. (1990): "Middle ear response in the chinchilla and its relationship to mechanics at the base of the cochlea," *J Acoust Soc Am* 87: 1612-1629
- Saunders J.C., Summers R.M. (1982): "Auditory structure and function in the mouse middle ear: An evaluation by SEM and capacitive probe," *J Comp Physiol* 146: 517-525
- Schawlow A.L., Townes C.H. (1958): "Infrared and optical masers," *Physical Review* 112: 1940-1949
- Schüssler M., Wörtge M. (1998): "Survey of excitation signals, with respect to scanning vibrometer measurements," (Polytec development department)
- Templer J., Davis W.E., Renner G.J., Thelin J.W. (1987): *Otolaryngology – Head and Neck Surgery: Principles and Concepts*, (Ishiyaku EuroAmerica, St. Louis)
- Tonndorf J., Khanna S.M. (1967): "Some properties of sound transmission in the middle and outer ears of cats," *J Acoust Soc Am* 41(2): 513-521
- Tonndorf J., Khanna S.M. (1972): "Tympanic-membrane vibrations in human cadaver ears studied by time-averaged holography," *J Acoust Soc Am* 52 (4 Pt 2): 1221-1233
- Vander A.J., Sherman J.H., Luciano D.S. (1994): *Human Physiology: The Mechanisms of Body Function*, 6th Edition (McGraw Hill, Sydney)
- Vogel U., Zahnert T., Hofmann G., Offergeld C., Hüttenbrink K.B. (1997): "Laser Vibrometry of the Middle Ear: Opportunities and Limitations," pp. 128-33 in Hüttenbrink K.B. (ed): *Middle ear mechanics in Research and Otosurgery. Proceedings of the International Workshop on Middle Ear Mechanics*, Dresden, Germany, 19-22 Sept, 1996. Dresden, University of Technology
- Voss S.E., Rosowski J.J., Merchant S.N., Peake W.T. (2000): "Acoustic responses of the human middle ear," *Hearing Research* 150: 43-69
- Wever E.G., Lawrence M. (1954): *Physiological Acoustics*. Princeton University Press, Princeton, NJ.

Willi U.B. (2003): "Middle-ear mechanics: The dynamic behavior of the incudo-malleolar joint and its role during the transmission of sound,"
http://www.unizh.ch/orl/diss_urban_willi.pdf

Zimmer W.M., Deborah F.R., Saunders J.C. (1994): "Middle-ear development VI: Structural maturation of the rat conducting apparatus," *Anatomical Record* 239: 475-484

emedicine.com. Homepage. Retrieved January 26, 2005.

<<http://www.emedicine.com/ent/byname/inner-ear-syndromic-sensorineural-hearing-loss.htm>>

thfc.ca. Homepage. The Hearing Foundation of Canada. Retrieved January 26, 2005.

<http://www.thfc.ca/news_plugs.html>